TABLE 1

AGS cDNAs isolated from cardiac hypertrophy model of mouse

AGSs are numbered according to the order in which they were isolated from a functional screen in yeast. GPR, G-protein-regulatory motif. The number of transformants screened for each cDNA library of the heart is as follows: transverse aortic constriction, 1.6×10^7; isoproterenol infusion, 2.0×10^7.

Gene in database	AGS	Cardiac dysfunction model used to generate cDNA libraries for functional screen[a]	
		Transverse aortic constriction	Isoproterenol infusion
Dynlt1b (the entire coding sequence)	AGS2	+	−
GPSM1 (C-terminal 178 amino acids with 3 GPR motifs)	AGS3	+	−
RGS12 (C-terminal 206 amino acids with GPR motif)	AGS6	+	+
TFE3 (C-terminal 533 amino acids)	AGS11	+	+
TFEB (C-terminal 320 amino acids)	AGS12	−	+
MITF (C-terminal 304 amino acids)	AGS13	+	+

[a] cDNA libraries were screened in yeast strains CY1141 ($G\alpha_{i3}$), CY8342 ($G\alpha_s$), and CY9603 ($G\alpha_{16}$).

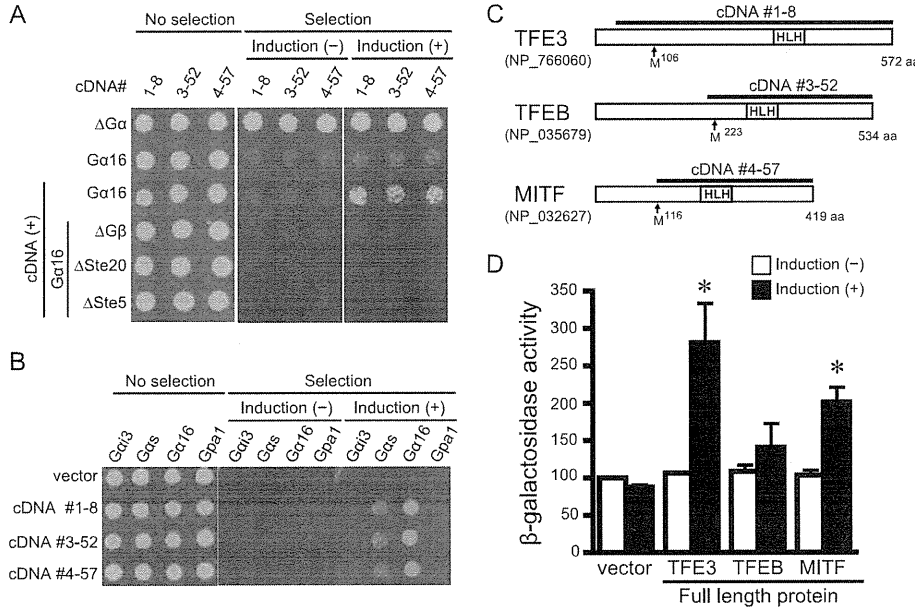

FIGURE 1. **Bioactivity and diagram of AGSs isolated from mouse hypertrophic heart.** In *A* and *B*, data are presented in three panels to illustrate the viability of the transformed yeast and the galactose-dependent growth under the selective pressure of exclusion of histidine from the medium. Galactose promotes the expression of each cDNA in the pYES2-containing *GAL1* promoter. About 2000 cells were suspended in H_2O and spotted on medium with glucose plus histidine (*left*; no selection), glucose minus histidine (*center*; selection without induction), or galactose plus histidine (*right*; selection plus induction). *A*, epistasis analysis of isolated clones. Transformants in a yeast strain expressing human $G\alpha_{16}$ (Gpa1(1–41)) and yeast lacking Gα, Gβ, or downstream signaling molecules (*ΔGα*, yeast lacking Gα; *ΔGβ*, yeast lacking Gβ; *ΔSte20*, yeast lacking p21-activated kinase; *ΔSte5*, yeast lacking the kinase scaffold protein). *B*, effect of isolated cDNAs in yeast expressing various types of Gα. *C*, schematic diagram of the sequences of TFE3, TFEB, and MITF in mouse. The *line above* the sequence refers to cDNA isolated by the yeast-based functional screen. *HLH*, helix-loop-helix. *D*, bioactivity of full-length TFE3, TFEB, and MITF. The full-length clones were transformed into yeast expressing $G\alpha_{16}$. The magnitude of activation of G-protein signaling pathway was monitored by β-galactosidase activity. Data are presented as the mean S.E. of five experiments with duplicate determinations. *, $p < 0.05$ *versus* non-induction group.

Miscellaneous Procedures and Statistical Analysis

Immunoblotting and data analysis were performed as described previously (18, 24). The luminescence images captured with an image analyzer (LAS-3000, Fujifilm, Tokyo, Japan) were quantified using Image Gauge 3.4 (Fujifilm). Data are expressed as mean ± S.E. from independent experiments as described in the figure legends. Statistical analyses were performed using the unpaired *t* test, F-test, and one-way analysis of variance followed by Tukey's multiple comparison post hoc test. All statistical analyses were performed with Prism 4 (GraphPad Software).

RESULTS

Identification of Activators of G-protein Signaling from Hypertrophied Hearts—We utilized an expression cloning system in *S. cerevisiae* to identify receptor-independent activators of G-protein signaling involved in the development of cardiac hypertrophy (18, 26). The yeast strains used in this screen system lacked the pheromone receptor but expressed mammalian Gα ($G\alpha_{i3}$, $G\alpha_s$, or $G\alpha_{16}$) in place of the yeast Gα subunit and provided a readout of growth upon activation of the G-protein-regulated pheromone signaling pathway. cDNA libraries from the left ventricle of the hypertrophy models were constructed in a galactose-inducible vector and introduced into these yeast strains. Functional screening for receptor-independent AGS proteins was then facilitated by selection of colonies growing in a galactose-specific manner.

We used two models of cardiac hypertrophy: the TAC-induced pressure overload model and the isoproterenol-induced tachycardiac hypertrophic model (supplemental Fig. 1). cDNA libraries from each model were introduced into the yeast strains expressing mammalian $G\alpha_{i3}$, $G\alpha_s$, or $G\alpha_{16}$ (Table 1). Twenty-

nine cDNA clones encoding six distinct proteins were isolated from the two cDNA libraries ($G\alpha_s$ strain, 0; $G\alpha_{i3}$ strain, 20; $G\alpha_{16}$ strain, 9). Each clone was retransformed into yeast to confirm plasmid-dependent growth, and then epistasis analysis was performed to identify the site of action within the pheromone pathway. Epistasis analysis demonstrated that six of these cDNA clones required G-protein to activate the growth-linked G-protein pathway, and thus these clones satisfied the definition of AGS (3, 27) (Table 1 and Fig. 1*A*).

Three clones isolated from yeast expressing $G\alpha_{i3}$ encoded the previously characterized proteins AGS2 (*Dynlt1b*, NCBI Reference Sequence NM_033368), AGS3 (*GPSM1*, NCBI Reference Sequence NM_700459), and AGS6 (*RGS12*, NCBI Reference Sequence NM_001156984). The cDNAs encoding AGS3 and AGS6 contained the G-protein-regulatory motif(s) that stabilizes the GDP-bound conformation of $G\alpha_i$, transducin, and $G\alpha_o$. An additional three cDNAs (1-8, 3-52, and 4-57) were isolated from yeast expressing $G\alpha_{16}$. These three cDNAs exhibited bioactivity in yeast strains expressing $G\alpha_{16}$ but not in yeast expressing $G\alpha_{i3}$, $G\alpha_s$, or Gpa1 (yeast $G\alpha$), indicating $G\alpha$ selectivity (Fig. 1*B* and supplemental Text 1). We therefore focused on these $G\alpha_{16}$-specific AGS cDNAs.

$G\alpha_{16}$-specific AGS Proteins—Sequence analysis of the $G\alpha_{16}$-specific cDNAs indicated that all encoded MITF/TFE transcription factors (31–33). cDNA1-8 encoded the C-terminal 533 amino acids of TFE3 (NCBI Reference Sequence NP_766060), cDNA3-52 encoded the C-terminal 320 amino acids of TFEB (NCBI Reference Sequence NP_035679), and cDNA4-57 encoded the C-terminal 304 amino acids of MITF (NCBI Reference Sequence NP_032627) (Fig. 1*C*). In accordance with the numbering of previously discovered AGS proteins (18), cDNA1-8, cDNA3-52, and cDNA4-57 were termed AGS11, AGS12, and AGS13, respectively (Table 1).

Full-length TFE3, TFEB, and MITF were cloned into a yeast expression vector, and the bioactivity for the G-protein signaling pathway was determined by β-galactosidase reporter assays (Fig. 1*D*). Full-length TFE3 and MITF, but not TFEB, activated the G-protein pathway in $G\alpha_{16}$-expressing cells. Full-length TFE3, MITF, and TFEB did not activate growth of yeast expressing $G\alpha_s$ (supplemental Text 2). Immunoblot analysis indicated that the full-length proteins were expressed at the

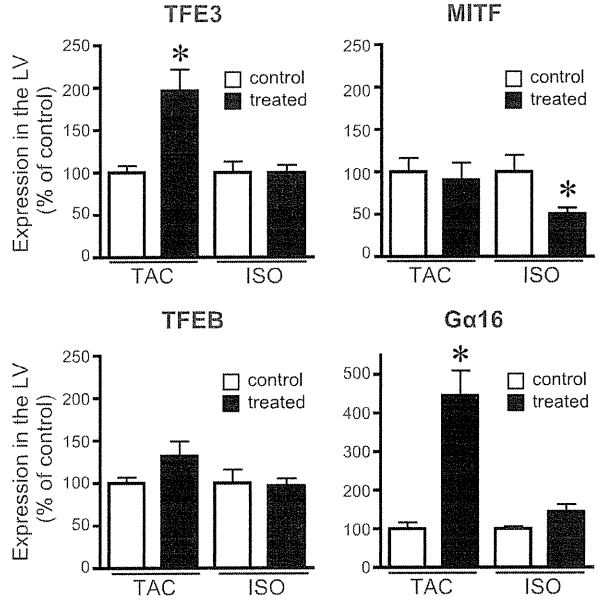

FIGURE 2. **Expression of MITF/TFE transcription factors and $G\alpha_{16}$ in mouse cardiac hypertrophy model.** The expression of mRNA of each gene was analyzed by real time PCR as described under "Experimental Procedures." *Control* refers to the sham-operated or saline-infused mouse. Data are expressed as the -fold change in level compared with the control group. *ISO*, continuous infusion of isoproterenol; *LV*, left ventricle. Data are presented as the mean ± S.E. of five experiments with duplicate determinations. *, $p < 0.05$ *versus* control group.

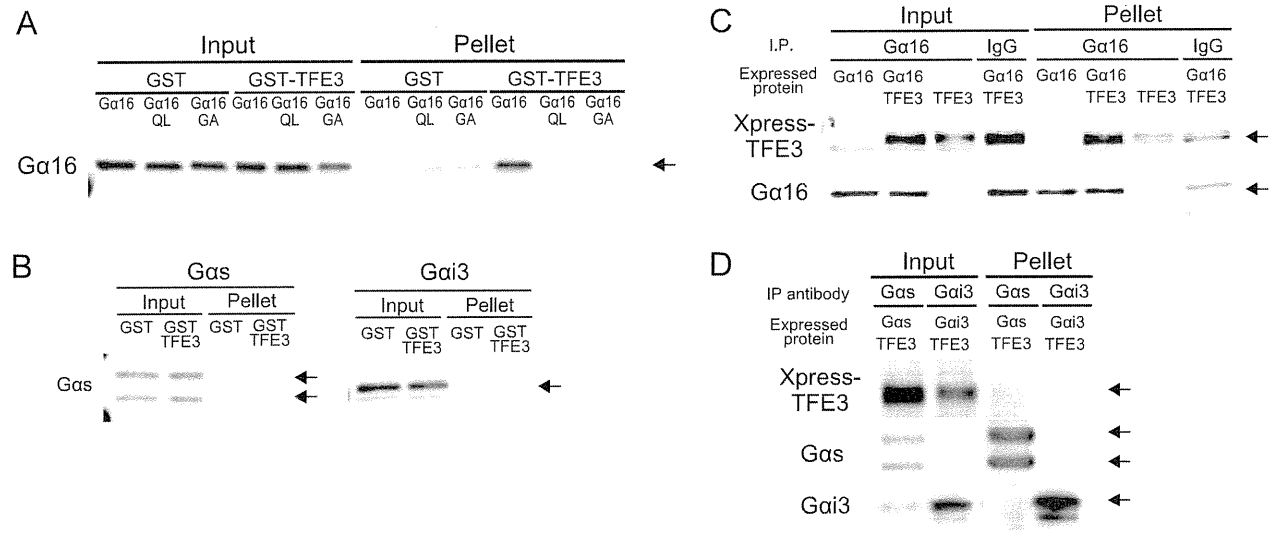

FIGURE 3. **Interaction of TFE3 with $G\alpha_{16}$ *in vitro* and in cell.** *A* and *B*, GST pulldown assay of TFE3 with COS7 lysate expressing various Gα subunits. The C-terminal 533-amino acid fragment of TFE3 was expressed as a GST fusion protein (GST-TFE3). GST-TFE3 (300 nM) was incubated with 1 mg of cell lysate in a total volume of 500 μl at 4 °C. Lysates of COS7 cells were prepared as described under "Experimental Procedures" following transfection of 10 μg of the Gα subunit in pcDNA3. *C* and *D*, COS7 cells in a 100-mm dish were transfected with a combination of pcDNA3, pcDNA3::$G\alpha_{16}$ (5 μg/dish), and pcDNA3.1-His::TFE3 (5 μg/dish). The amount of DNA transfected was adjusted to 10 μg/well with the pcDNA3 vector. The preparation of a whole-cell lysate including the nuclear fraction and immunoprecipitation (*IP*) were performed as described under "Experimental Procedures." The Gα subunit was immunoprecipitated with a specific antibody for each Gα subunit. *QL*, $G\alpha_{16}$Q212L; *GA*, $G\alpha_{16}$G211A.

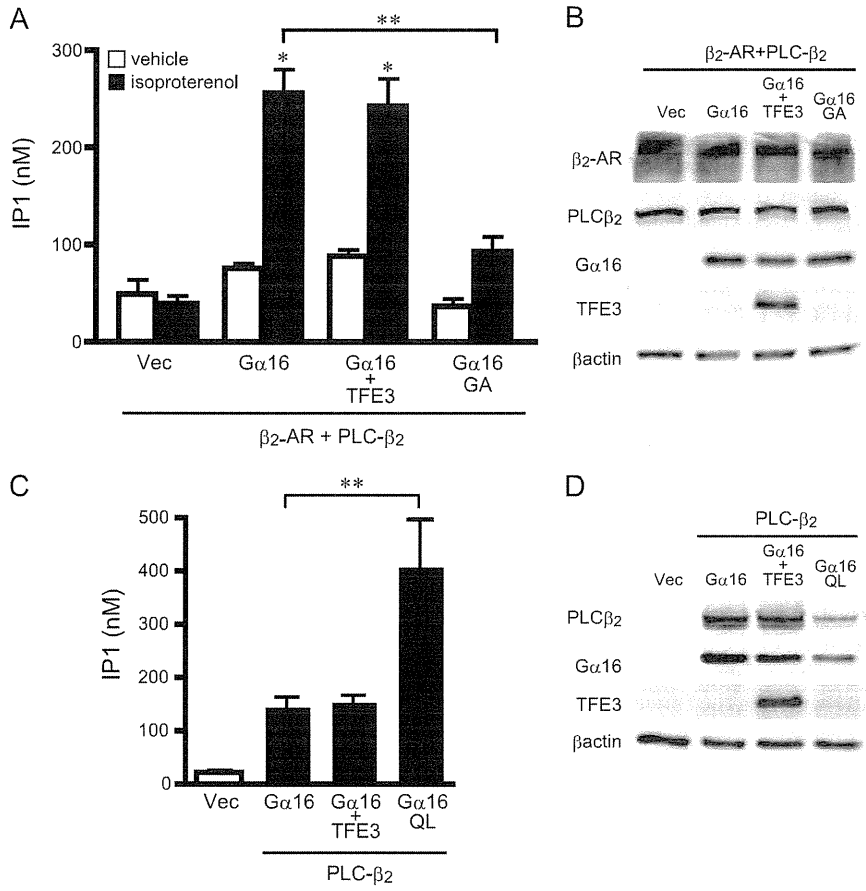

FIGURE 4. **Effect of TFE3 on activation of phospholipase C-β2.** *A*, effect of TFE3 on the generation of inositol phosphate (*IP1*) following receptor stimulation. COS7 cells were transfected in 12-well plates with control vectors (*Vec*) or cDNAs as indicated (0.4 μg of pcDNA::PLC-β2, 0.5 μg of pcDNA::TFE3, 0.5 μg of pcDNA::$G\alpha_{16}$, and 0.6 μg of pEGFP::β_2-adrenergic receptor (*AR*)). The amount of transfected DNA was adjusted to 2 μg/well with the pcDNA vector. Cells were stimulated with 10 μM isoproterenol for 30 min and assayed immediately. Data are expressed as the mean ± S.E. of five experiments with duplicate determinations. *B*, expression of transfected proteins of *A*. The expression of each protein was determined by immunoblotting of 10 μg of whole-cell lysates. *C*, effect of TFE3 on the generation of inositol phosphate. COS7 cells were transfected in 12-well plates with control vectors or cDNAs as indicated (0.5 μg of pcDNA::PLC-β2, 0.75 μg of pcDNA::TFE3, and 0.75 μg of pcDNA::$G\alpha_{16}$). The amount of transfected DNA was adjusted to 2 μg/well with the pcDNA vector. Data are expressed as the mean ± S.E. of five experiments with duplicate determinations. *D*, expression of transfected cDNA of *C*. The expression of each protein was determined by immunoblotting of 10 μg of whole-cell lysates. *, $p < 0.05$ *versus* control group; **, $p < 0.05$ between two groups. *QL*, $G\alpha_{16}$Q212L; *GA*, $G\alpha_{16}$G211A.

expected size and that their expression did not alter the levels of $G\alpha_{16}$. These findings suggest that TFE3, MITF, and TFEB are transcription factors that act as receptor-independent G-protein activators. AGSs with various functions have been identified; however, no transcription factors have previously been described as AGS proteins.

Expression of TFE3, TFEB, and MITF in Cardiac Hypertrophy Models—It was reported previously that the expression level of MITF was associated with development of cardiac hypertrophy in mouse (34). We sought to determine whether the three $G\alpha_{16}$-specific AGS proteins were up-regulated in cardiac hypertrophy or were constitutively expressed in the myocardium. RNA expression of TFE3, MITF, TFEB, and the target $G\alpha_{16}$ subunit was determined in the hypertrophied myocardium (Fig. 2). TFE3 mRNA expression was up-regulated in the left ventricle in the TAC model but not in the isoproterenol model. MITF was unchanged in the TAC model but reduced in the isoproterenol model. TFEB did not show any significant changes of expression in either model. Notably, $G\alpha_{16}$ mRNA expression was also increased in the TAC model in which TFE3 was up-regulated. As TFE3 and $G\alpha_{16}$ were both significantly up-regulated in the TAC model, we focused on the characterization of TFE3.

Formation of TFE3-$G\alpha_{16}$ Complex in Cells—The above findings suggested that TFE3 plays an important role via $G\alpha_{16}$ in the development of cardiac hypertrophy. We thus examined whether TFE3 indeed was able to form a complex with $G\alpha_{16}$. As a first approach, the interaction of GST-tagged TFE3 (GST-TFE3) with $G\alpha_{16}$ was examined *in vitro*. GST-TFE3 successfully pulled down transfected $G\alpha_{16}$ from cell lysates. However, neither a constitutively active mutant of $G\alpha_{16}$ ($G\alpha_{16}$Q212L) nor an inactive mutant of $G\alpha_{16}$ ($G\alpha_{16}$G211A) was pulled down, suggesting that the interaction of $G\alpha_{16}$ and TFE3 was dependent upon the conformation of $G\alpha_{16}$ and regulated by guanine nucleotide binding (Fig. 3*A*) (35, 36). In contrast, GST-TFE3 did not pull down transfected $G\alpha_s$ or $G\alpha_{i3}$ from cell lysates (Fig. 3*B*). We also examined whether TFE3 interacted with $G\alpha_{16}$ in mammalian cells. Expressed TFE3 was co-immunoprecipitated with $G\alpha_{16}$ from COS7 cell lysates, suggesting that TFE3 and $G\alpha_{16}$ formed a stable complex

within these cells (Fig. 3*C*). In contrast, TFE3 did not co-immunoprecipitate with $G\alpha_s$ or $G\alpha_{i3}$ (Fig. 3*D*). We next examined the role of this interaction in $G\alpha_{16}$-mediated signaling events.

TFE3 Is Not Involved in Receptor-mediated $G\alpha_{16}$ Signaling—$G\alpha_{16}$ is coupled to multiple GPCRs including β_2-adrenergic receptors mediating signal transfer to the effector molecule PLC-β (37, 38). Thus, we examined whether TFE3 regulated β_2-adrenergic receptor-mediated PLC-β2 activation as a representative of $G\alpha_{16}$-mediated signaling (39). In a transient expression system in COS7 cells, $G\alpha_{16}$ activated PLC-β2 following β_2-adrenergic receptor stimulation as determined by inositol monophosphate production (Fig. 4). The magnitude of PLC-β2 activation was reduced in the presence of an inactive $G\alpha_{16}$ mutant ($G\alpha_{16}$G211A), indicating that PLC-β2 activation was mediated by $G\alpha_{16}$ (Fig. 4, *A* and *B*). However, TFE3 overexpression did not alter this receptor-mediated $G\alpha_{16}$ signaling. We also examined the effect of TFE3 overexpression on the basal activity of PLC-β2/$G\alpha_{16}$ in the absence of receptor stimulation. TFE3 overexpression did not alter PLC-β2 activity, whereas a constitutively active mutant of $G\alpha_{16}$ ($G\alpha_{16}$Q212L) increased the activity even in the absence of receptor stimulation (Fig. 4, *C* and *D*). These data are consistent with a lack of TFE3 involvement in regulating the conventional GPCR-mediated $G\alpha_{16}$ signaling pathway.

TFE3 Induces Accumulation of $G\alpha_{16}$ in Nucleus—The identification of transcription factors as $G\alpha_{16}$-specific AGS proteins suggested that MITF/TFE transcription factors may interact with a subpopulation of $G\alpha_{16}$ distinct from that involved in the conventional G-protein signaling at the plasma membrane. To address this issue, we first examined the subcellular distribution of $G\alpha_{16}$ and TFE3 when each was independently overexpressed in the cell. Overexpressed TFE3 was predominantly found in the nucleus as expected, whereas $G\alpha_{16}$ was found in the plasma membrane and cytoplasm but not in the nucleus (Fig. 5, *arrow*, and supplemental Fig. 2, A, B, and D). However, when $G\alpha_{16}$ and TFE3 were overexpressed together, $G\alpha_{16}$ predominantly accumulated in the nucleus (Fig. 5, *arrow*). This novel nuclear translocation of $G\alpha_{16}$ was not due to $G\alpha_{16}$ activation because the constitutively active mutant of $G\alpha_{16}$ ($G\alpha_{16}$Q212L) was not found in the nucleus when it was overexpressed by itself. These data suggested that $G\alpha_{16}$ forms a complex with TFE3 and translocates to the nucleus. Nuclear accumulation of G-protein by TFE3 was not observed for $G\alpha_{i3}$ or $G\alpha_s$.

Up-regulation of Claudin 14 mRNA by TFE3-$G\alpha_{16}$ Complex—The co-localization of TFE3 and $G\alpha_{16}$ suggested an involvement of a nuclear TFE3-$G\alpha_{16}$ complex in regulating the expression of particular genes. To address this issue, genes regulated by TFE3 and $G\alpha_{16}$ were screened by microarray analysis of mRNA of HEK293 cells transfected with TFE3 and/or $G\alpha_{16}$. In the screening of more than 40,000 human genes, we found that claudin 14 mRNA was highly up-regulated by the simultaneous transfection of TFE3 and $G\alpha_{16}$. Parallel experiments indicated that the co-overexpression of TFE3 and $G\alpha_{16}$ in HEK293 cells increased claudin 14 mRNA by 133-fold, whereas independent overexpression of TFE3 (8.3-fold) or $G\alpha_{16}$ (1.0-fold) had minimal effect on the induction of claudin 14 (Fig. 6*A*). The induction of claudin 14 was significantly decreased in the presence of the inactive mutant of $G\alpha_{16}$ ($G\alpha_{16}$G211A) compared with wild type $G\alpha_{16}$, suggesting that $G\alpha_{16}$ activation was also required for the induction of this gene.

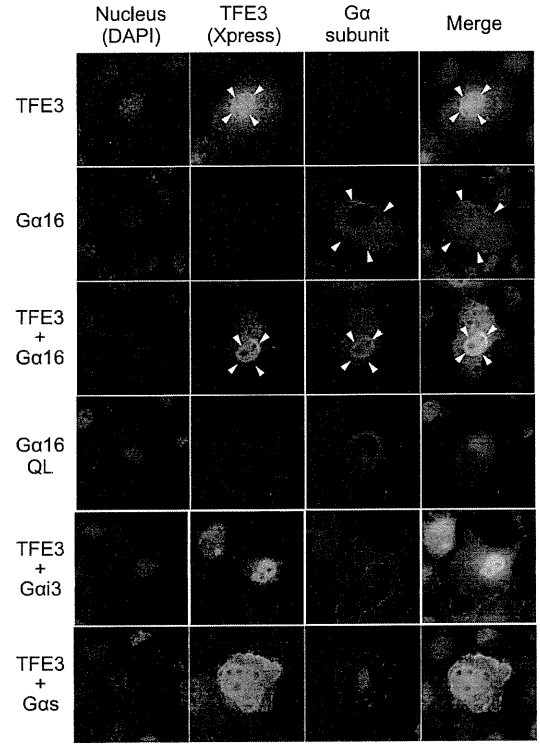

FIGURE 5. **Localization of expressed Gα subunits and TFE3 in COS7 cells.** COS7 cells were transfected in a 35-mm dish with 2.0 μg of Gα subunits in pcDNA3 and/or 2.0 μg of pcDNA3.1-His::TFE3. The amount of transfected DNA was adjusted to 4 μg/well with the pcDNA3 vector. The Gα subunit and TFE3 were determined using a specific antibody for each Gα (*red*) or Xpress antibody (*green*), respectively. *QL*, $G\alpha_{16}$Q212L.

Requirement of $G\alpha_{16}$ Activation for Gene Induction by TFE3—The requirement of $G\alpha_{16}$ activation for this gene induction was further characterized utilizing a truncated mutant of TFE3 (delTFE3), which showed less bioactivity for $G\alpha_{16}$ activation in the yeast system. Analysis of the amino acid sequences of the MITF/TFE family indicated that the C-terminal 27 acids were conserved among the $G\alpha_{16}$-selective AGS proteins (Fig. 6*B*, *upper panel*). Deletion of the C-terminal 27 amino acids resulted in the loss of bioactivity of TFE3 and MITF for G-protein activation (Fig. 6*B*, *left middle panel*, and supplemental Text 3). Despite the loss of bioactivity for $G\alpha_{16}$ activation, delTFE3 was still able to form a complex with $G\alpha_{16}$ and induce the translocation of $G\alpha_{16}$ to the nucleus (Fig. 6*B*, *left lower* and *right panels*, and supplemental Fig. 2, C and D). Thus, nuclear translocation by itself did not require $G\alpha_{16}$ activation as long as TFE3 and $G\alpha_{16}$ formed a complex (Fig. 6*A*).

Although the delTFE3-$G\alpha_{16}$ complex was found in the nucleus, the subsequent up-regulation of claudin 14 was blunted, suggesting that $G\alpha_{16}$ activation is critical for this gene induction (Fig. 6*A*). Furthermore, the constitutively active mutant of $G\alpha_{16}$ ($G\alpha_{16}$Q212L), which was not expressed in the nucleus (Fig. 5), failed to induce claudin 14. MITF, which had a similar ability to activate $G\alpha_{16}$ (Fig. 1*D*), failed to induce claudin

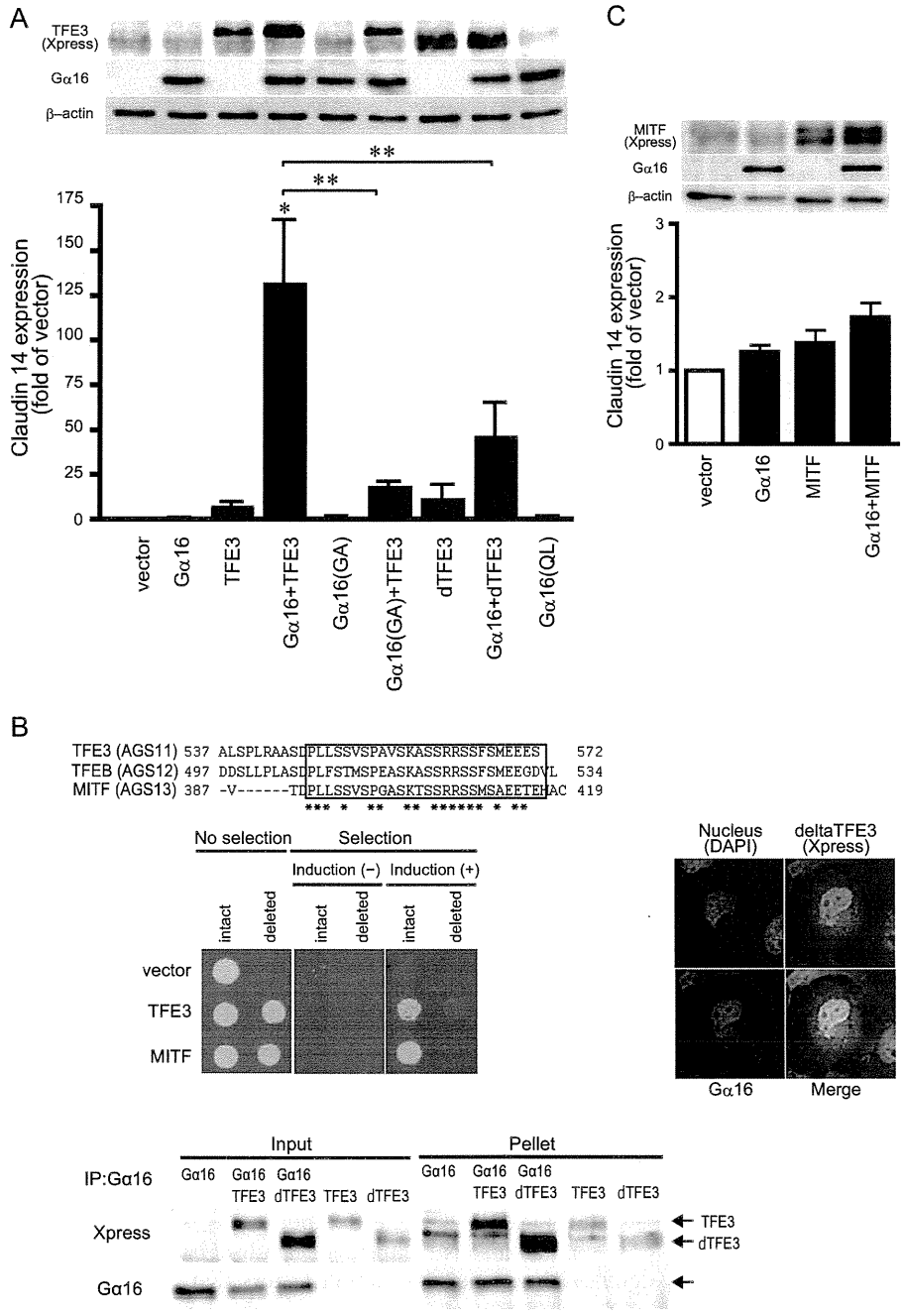

FIGURE 6. **Effect of TFE3 or MITF on expression of claudin 14.** *A*, expression of claudin 14 in transfected HEK293 cells. HEK293 cells were transfected in 6-well plates with a combination of control vectors or cDNAs as indicated (2.0 μg of Gα subunits in pcDNA3 and 2.0 μg of TFE3 or delTFE3 in pcDNA3.1-His). The amount of transfected DNA was adjusted to 4 μg/well with the pcDNA3 vector. The expression of claudin 14 mRNA was analyzed by real time PCR. Data are expressed as the -fold change from the level of claudin 14 expression in control cells transfected with the vector alone. Data are expressed as the mean ± S.E. of five experiments with duplicate determinations. *Upper inset*, expression of proteins determined by immunoblotting (~10 μg of whole-cell lysate). Data are representative of five experiments. *, $p < 0.05$ *versus* control group; **, $p < 0.05$ between two groups. *B*, effect of delTFE3. *Upper panel*, amino acid sequence of C-terminal MITF/TFE transcription factors. The *square* indicates conserved amino acid sequence. *, consensus amino acid. *Middle left panel*, bioactivity of intact or deleted TFE3 in yeast expressing $G\alpha_{16}$. The assay was performed as described under "Experimental Procedures." *Middle right panel*, localization of transfected $G\alpha_{16}$ and TFE3 in COS7 cells. COS7 cells were transfected in a 35-mm dish with 2.0 μg of pcDNA3::$G\alpha_{16}$ and 2.0 μg of pcDNA3.1-His::TFE3. $G\alpha_{16}$ and TFE3 were determined using $G\alpha_{16}$ antibody (*red*) or Xpress antibody (*green*), respectively. *Lower panel*, interaction of $G\alpha_{16}$ with TFE3 or delTFE3. COS7 cells in a 100-mm dish were transfected with a combination of pcDNA3, pcDNA3::$G\alpha_{16}$ (5 μg/dish), pcDNA3.1-His::TFE3 (5 μg/dish), and pcDNA3.1-His::delTFE3 (5 μg/dish). The amount of transfected DNA was adjusted to 10 μg/well with the pcDNA3 vector. The preparation of the cell lysate and immunoprecipitation (*IP*) were performed as described under "Experimental Procedures". *C*, effect of MITF on claudin 14 expression in transfected HEK293 cells. HEK293 cells were transfected in 6-well plates with a combination of control vectors or cDNAs as indicated (2.0 μg of pcDNA3::$G\alpha_{16}$ and 2.0 μg of pcDNA3.1-His::MITF). The amount of transfected DNA was adjusted to 4 μg/well with the pcDNA3 vector. The expression of claudin 14 mRNA was analyzed by real time PCR. Data are expressed as the -fold change in the level of claudin 14 in control cells transfected with the vector alone. Data are expressed as the mean ± S.E. of five experiments with duplicate determinations. *Upper inset*, expression of proteins determined by immunoblotting (~10 μg of whole-cell lysate). Data are representative of five experiments. *QL*, $G\alpha_{16}$Q212L; *GA*, $G\alpha_{16}$G211A.

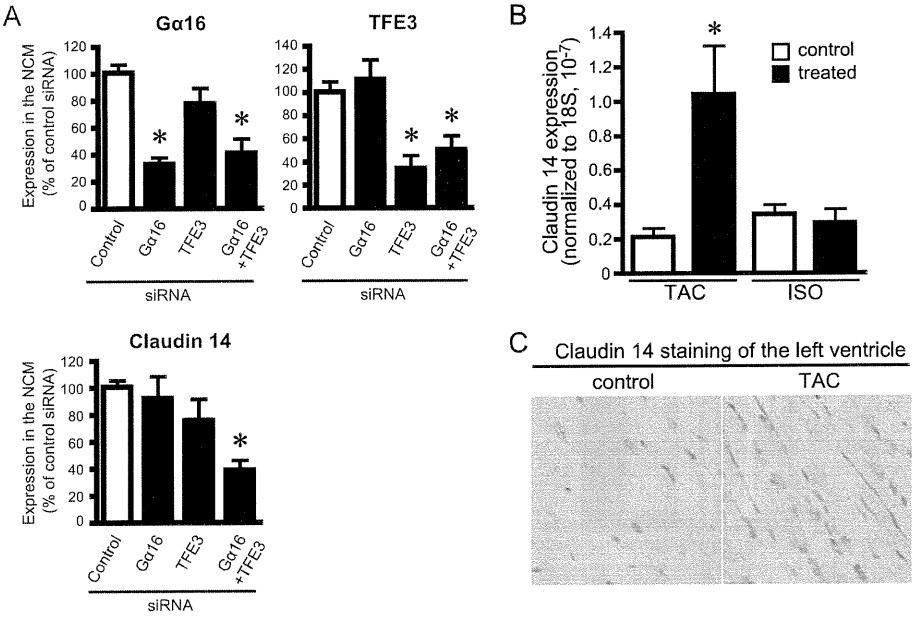

FIGURE 7. **Expression of claudin 14 in cultured cardiomyocytes and hypertrophied heart.** *A*, effect of knockdown of $G\alpha_{16}$ and TFE3 on the level of claudin 14 mRNA in cultured cardiomyocytes. Neonatal cardiomyocytes (*NCM*) were transfected with each siRNA and/or universal control siRNA (Stealth RNAi Negative Control, Invitrogen). Forty-eight hours after transfection, the level of mRNA of $G\alpha_{16}$ (*A*), TFE3 (*B*), and claudin 14 (*C*) were analyzed by real time PCR. Transfection efficiency of siRNA was estimated at 70–80% using FITC-labeled double strand RNA (Block It Fluorescent Oligo, Invitrogen) (*right panel*). *, $p < 0.05$ *versus* negative siRNA. Data are expressed as the mean ± S.E. of seven to eight independent experiments. *B* and *C*, expression of claudin 14 in the mouse cardiac hypertrophy model. *B*, the left ventricular expression of claudin 14 mRNA was analyzed by real time PCR. *Control* refers to the sham-operated or saline-infused mouse. Data are expressed as the -fold change in claudin 14 level from that in control group. Data are expressed as the mean ± S.E. of five experiments with duplicate determinations. *C*, immunohistochemical staining for claudin 14 (1:100; *brown*) of the left ventricle of sham- or TAC-operated mouse. A frozen section (8 μm) of the mouse heart was subjected to immunohistochemical staining as described under "Experimental Procedures". *Blue*, nucleus. *ISO*, continuous infusion of isoproterenol. *, $p < 0.05$ *versus* control group.

14 (Fig. 6*C*). Taken together, the results suggest that in addition to the nuclear translocation of a TFE3-$G\alpha_{16}$ complex activation of $G\alpha_{16}$ in the nucleus was required for the induction of claudin 14.

Regulation of Claudin 14 Expression in Cardiomyocytes—The influence of $G\alpha_{16}$ and TFE3 on the expression of claudin 14 was also examined in neonatal cardiomyocytes following knockdown of $G\alpha_{16}$ and/or TFE3 by siRNA. $G\alpha_{16}$siRNA or TFE3siRNA successfully suppressed the level of target molecules to 33–34% of the level of cardiomyocytes treated with negative control siRNA (Fig. 7*A*). The level of claudin 14 in cardiomyocytes was not influenced by $G\alpha_{16}$siRNA or TFE3siRNA itself when they were separately introduced (Fig. 7*A*, *lower panel*). However, interestingly, the simultaneous knockdown of $G\alpha_{16}$ and TFE3 by siRNAs significantly reduced the claudin 14 mRNA (38.9 ± 7.4%, $p < 0.05$ *versus* control siRNA), indicating that both $G\alpha_{16}$ and TFE3 were required for the regulation claudin 14 expression. These results are consistent with the data observed in HEK293 cells.

Up-regulation of Claudin 14 in Mouse Heart upon Pressure Overload Stress—As TFE3 and $G\alpha_{16}$ were simultaneously up-regulated in the left ventricle in the TAC model (Fig. 2), we examined whether ventricular claudin 14 was also up-regulated in the models of cardiac hypertrophy. Quantitative PCR analysis indicated that claudin 14 mRNA was increased 5-fold in the left ventricle in the TAC model but not in the isoproterenol model of cardiac hypertrophy (Fig. 7*B*), consistent with the expression profile of TFE3 and $G\alpha_{16}$ in these stimulated models (Fig. 2). Immunocytochemical analysis indicated that expression of claudin 14 was increased in the lateral membrane of cardiomyocytes rather than the intercalated disks (Fig. 7*C*). Thus, similar to our findings in cultured cells, the simultaneous up-regulation of TFE3 and $G\alpha_{16}$ was associated with gene induction of claudin 14 *in vivo* under pathologic conditions. Gene induction by $G\alpha_{16}$ and TFE3 is therefore postulated to be part of the cardiac adaptation process to pressure overload stress.

DISCUSSION

We report the identification of three MITF/TFE transcription factors, TFE3, MITF, and TFEB, as new AGS proteins selective for the $G\alpha_{16}$ subunit. These factors belong to the Myc supergene family of basic helix-loop-helix leucine zipper transcription factors that act either as a homo- or heterodimer within the family members (31–33). TFE3 formed a complex with and activated $G\alpha_{16}$ in cells. Formation of TFE3-$G\alpha_{16}$ complex resulted in the translocation of $G\alpha_{16}$ to the nucleus and up-regulation of the cell junction protein claudin 14. Expression of claudin 14 was also induced *in vivo* in the hypertrophied ventricle, and this was associated with the up-regulation of $G\alpha_{16}$ and TFE3. Thus, the transcription factor TFE3 is postulated to act as a G-protein activator for the $G\alpha_{16}$ subunit and regulate gene induction in response to pathophysiologic stress.

Although an increasing body of data implicates heterotrimeric G-proteins and their regulators as key regulators in multiple cellular events (40, 41), this is the first demonstration that activation of a Gα subunit by an AGS drives relocalization of Gα to the nucleus and gene transcription in mammalian cells.

Previous studies reported that heterotrimeric $G\beta_5$ translocated to the nucleus when complexed with RGS7 (16). However, the effect of RGS7-$G\beta_5$ on gene regulation has not yet been characterized. This study is the first to demonstrate a direct effect of nuclear translocation of a $G\alpha$ subunit on specific gene regulation.

The magnitude of gene induction by TFE3-$G\alpha_{16}$ was clearly dependent on the guanine nucleotide binding status of $G\alpha_{16}$ as well as the bioactivity of TFE3 for $G\alpha_{16}$ activation. Activation of $G\alpha_{16}$ in the cytosol or plasma membrane was not sufficient to induce claudin 14 expression because a constitutively active $G\alpha_{16}$ in the cytosol and plasma membrane failed to induce claudin 14 expression. Conversely, translocation of $G\alpha_{16}$ to the nucleus by the delTFE3, which lacked the ability to activate $G\alpha_{16}$, showed a blunted induction of claudin 14 as compared with intact TFE3. These observations suggest that TFE3-mediated activation of $G\alpha_{16}$ within the nucleus is essential to induce claudin 14 expression. TFE3 may serve as a direct guanine nucleotide exchange factor for $G\alpha_{16}$ upon complex formation. Alternatively, $G\alpha_{16}$ may be activated in the nucleus following removal or addition of a factor to the TFE3 complex when it is translocated into the nucleus.

The up-regulation of claudin 14 reported in this study may be an important event in remodeling of the heart following pressure overload stress. Claudin 14 was expressed in the lateral membrane of cardiomyocytes and was increased upon pressure overload stress. Claudin 14 is a member of the claudin family of more than 20 highly conserved proteins (42–44). It is interesting that the overexpression of claudin 14 induces apoptosis of cells independently of the caspase-mediated pathway (45). Moreover, in addition to its barrier function, claudin is also involved in activating pro-matrix metalloproteinase 2, which plays a role in reorganization of the extracellular matrix (46). Accordingly, the claudin-mediated sealing and/or molecular remodeling of the lateral region where cardiomyocytes are associated with the basal lamina or extracellular matrix is important for adaptation to mechanical stress. Indeed, changes in the expression of claudin 5 have been reported in the lateral membrane of cardiomyocytes in a dystrophic mouse with dilated cardiomyopathy (47, 48).

It is possible that the transcription factor MITF/TFE acts as a heterologous protein complex and binds to promoter regions to regulate the transcription of claudin 14. TFE3-$G\alpha_{16}$ may be required to assemble such a transcriptional complex, leading to increased transcription. Alternatively, TFE3-$G\alpha_{16}$ may regulate nuclear PLC-β activity and the nuclear phosphoinositide cycle independently of the plasma membrane phosphoinositide cycle influencing cell cycle and cell differentiation (49). Activation of PLC-β in the nucleus is not usually detectable in whole-cell experiments as used in this study (Fig. 4).

This is the first report of a regulatory protein for the $G\alpha_{16}$ subunit, which can be coupled to multiple GPCRs in a variety of experimental systems (37, 38). Although $G\alpha_{16}$ is enriched in hematopoietic tissue, it is also expressed in other tissues including heart (50, 51) where its expression is increased 4-fold by the cardiac stress induced in the TAC animal model. It is of particular interest to find that this multifunctional $G\alpha_{16}$ is translocated into the nucleus by a specific G-protein regulator where it plays a previously unappreciated functional role.

Various AGS proteins are involved in adaptation to various pathologic conditions (3, 20). For example, we previously identified AGS8 as a novel regulatory protein for the $G\beta\gamma$ subunit in a repetitive transient ischemia model in the rat heart (18). AGS8 was up-regulated in the myocardium by ischemic/hypoxic stress and played a critical role in hypoxia-induced apoptosis of cardiomyocytes (18, 24). Our ability to rapidly identify AGS8 and now TFE3 directly from disease-specific mRNA libraries using our yeast-based functional screen highlights its usefulness in discovering disease-specific regulatory proteins for heterotrimeric G-proteins. Such disease-specific or adaptation-specific regulatory proteins represent novel therapeutic targets in treating human diseases.

Acknowledgments—We acknowledge Dr. James R. Broach (Molecular Biology, Princeton University, Princeton, NJ) and Cadus Pharmaceutical Corp. (New York, NY) for providing yeast strains used in this study. We thank Dr. Kazuhiro Ogata (Biochemistry and Gene Regulation, Yokohama City University) for helpful comments.

REFERENCES

1. Birnbaumer, L. (2007) *Biochim. Biophys. Acta* **1768,** 772–793
2. Oldham, W. M., and Hamm, H. E. (2006) *Q. Rev. Biophys.* **39,** 117–166
3. Sato, M., Blumer, J. B., Simon, V., and Lanier, S. M. (2006) *Annu. Rev. Pharmacol. Toxicol.* **46,** 151–187
4. Cismowski, M. J. (2006) *Semin. Cell Dev. Biol.* **17,** 334–344
5. Blumer, J. B., Smrcka, A. V., and Lanier, S. M. (2007) *Pharmacol. Ther.* **113,** 488–506
6. Riddle, E. L., Schwartzman, R. A., Bond, M., and Insel, P. A. (2005) *Circ. Res.* **96,** 401–411
7. Tall, G. G., and Gilman, A. G. (2005) *Proc. Natl. Acad. Sci. U.S.A.* **102,** 16584–16589
8. Lee, M. J., and Dohlman, H. G. (2008) *Curr. Biol.* **18,** 211–215
9. Garcia-Marcos, M., Ghosh, P., and Farquhar, M. G. (2009) *Proc. Natl. Acad. Sci. U.S.A.* **106,** 3178–3183
10. Willars, G. B. (2006) *Semin. Cell Dev. Biol.* **17,** 363–376
11. Du, Q., Stukenberg, P. T., and Macara, I. G. (2001) *Nat. Cell Biol.* **3,** 1069–1075
12. Gotta, M., Dong, Y., Peterson, Y. K., Lanier, S. M., and Ahringer, J. (2003) *Curr. Biol.* **13,** 1029–1037
13. Sanada, K., and Tsai, L. H. (2005) *Cell* **122,** 119–131
14. Blumer, J. B., Kuriyama, R., Gettys, T. W., and Lanier, S. M. (2006) *Eur. J. Cell Biol.* **85,** 1233–1240
15. Shu, F. J., Ramineni, S., Amyot, W., and Hepler, J. R. (2007) *Cell. Signal.* **19,** 163–176
16. Hepler, J. R. (2005) *Sci. STKE* **2005,** pe38
17. Sato, M., Gettys, T. W., and Lanier, S. M. (2004) *J. Biol. Chem.* **279,** 13375–13382
18. Sato, M., Cismowski, M. J., Toyota, E., Smrcka, A. V., Lucchesi, P. A., Chilian, W. M., and Lanier, S. M. (2006) *Proc. Natl. Acad. Sci. U.S.A.* **103,** 797–802
19. Blumer, J. B., Lord, K., Saunders, T. L., Pacchioni, A., Black, C., Lazartigues, E., Varner, K. J., Gettys, T. W., and Lanier, S. M. (2008) *Endocrinology* **149,** 3842–3849
20. Sato, M., and Ishikawa, Y. (2010) *Pathophysiology* **17,** 89–99
21. Hendriks-Balk, M. C., Peters, S. L., Michel, M. C., and Alewijnse, A. E. (2008) *Eur. J. Pharmacol.* **585,** 278–291
22. Heximer, S. P., Srinivasa, S. P., Bernstein, L. S., Bernard, J. L., Linder, M. E., Hepler, J. R., and Blumer, K. J. (1999) *J. Biol. Chem.* **274,** 34253–34259
23. Rogers, J. H., Tamirisa, P., Kovacs, A., Weinheimer, C., Courtois, M., Blumer, K. J., Kelly, D. P., and Muslin, A. J. (1999) *J. Clin. Investig.* **104,**

567–576
24. Sato, M., Jiao, Q., Honda, T., Kurotani, R., Toyota, E., Okumura, S., Takeya, T., Minamisawa, S., Lanier, S. M., and Ishikawa, Y. (2009) *J. Biol. Chem.* **284,** 31431–31440
25. Hill, J. A., Karimi, M., Kutschke, W., Davisson, R. L., Zimmerman, K., Wang, Z., Kerber, R. E., and Weiss, R. M. (2000) *Circulation* **101,** 2863–2869
26. Cismowski, M. J., Takesono, A., Ma, C., Lizano, J. S., Xie, X., Fuernkranz, H., Lanier, S. M., and Duzic, E. (1999) *Nat. Biotechnol.* **17,** 878–883
27. Takesono, A., Cismowski, M. J., Ribas, C., Bernard, M., Chung, P., Hazard, S., 3rd, Duzic, E., and Lanier, S. M. (1999) *J. Biol. Chem.* **274,** 33202–33205
28. Cismowski, M. J., Takesono, A., Ma, C., Lanier, S. M., and Duzic, E. (2002) *Methods Enzymol.* **344,** 153–168
29. Sato, M., Ribas, C., Hildebrandt, J. D., and Lanier, S. M. (1996) *J. Biol. Chem.* **271,** 30052–30060
30. Sato, M., Kataoka, R., Dingus, J., Wilcox, M., Hildebrandt, J. D., and Lanier, S. M. (1995) *J. Biol. Chem.* **270,** 15269–15276
31. Hodgkinson, C. A., Moore, K. J., Nakayama, A., Steingrímsson, E., Copeland, N. G., Jenkins, N. A., and Arnheiter, H. (1993) *Cell* **74,** 395–404
32. Hughes, M. J., Lingrel, J. B., Krakowsky, J. M., and Anderson, K. P. (1993) *J. Biol. Chem.* **268,** 20687–20690
33. Steingrímsson, E., Copeland, N. G., and Jenkins, N. A. (2004) *Annu. Rev. Genet.* **38,** 365–411
34. Tshori, S., Gilon, D., Beeri, R., Nechushtan, H., Kaluzhny, D., Pikarsky, E., and Razin, E. (2006) *J. Clin. Investig.* **116,** 2673–2681
35. Heasley, L. E., Storey, B., Fanger, G. R., Butterfield, L., Zamarripa, J., Blumberg, D., and Maue, R. A. (1996) *Mol. Cell. Biol.* **16,** 648–656
36. Zhou, J., Stanners, J., Kabouridis, P., Han, H., and Tsoukas, C. D. (1998) *Eur. J. Immunol.* **28,** 1645–1655
37. Huang, J., and Wilkie, T. M. (2006) *UCSD-Nature Molecule Pages* 10.1038/mp.a000972.01
38. Offermanns, S., and Simon, M. I. (1995) *J. Biol. Chem.* **270,** 15175–15180
39. Wu, D., Kuang, Y., Wu, Y., and Jiang, H. (1995) *J. Biol. Chem.* **270,** 16008–16010
40. Burchett, S. A. (2003) *J. Neurochem.* **87,** 551–559
41. Spiegelberg, B. D., and Hamm, H. E. (2007) *Curr. Opin. Genet. Dev.* **17,** 40–44
42. Tsukita, S., and Furuse, M. (2002) *Curr. Opin. Cell Biol.* **14,** 531–536
43. Wilcox, E. R., Burton, Q. L., Naz, S., Riazuddin, S., Smith, T. N., Ploplis, B., Belyantseva, I., Ben-Yosef, T., Liburd, N. A., Morell, R. J., Kachar, B., Wu, D. K., Griffith, A. J., Riazuddin, S., and Friedman, T. B. (2001) *Cell* **104,** 165–172
44. Ben-Yosef, T., Belyantseva, I. A., Saunders, T. L., Hughes, E. D., Kawamoto, K., Van Itallie, C. M., Beyer, L. A., Halsey, K., Gardner, D. J., Wilcox, E. R., Rasmussen, J., Anderson, J. M., Dolan, D. F., Forge, A., Raphael, Y., Camper, S. A., and Friedman, T. B. (2003) *Hum. Mol. Genet.* **12,** 2049–2061
45. Hu, Y., Lehrach, H., and Janitz, M. (2010) *Mol. Biol. Rep.* **37,** 3381–3387
46. Miyamori, H., Takino, T., Kobayashi, Y., Tokai, H., Itoh, Y., Seiki, M., and Sato, H. (2001) *J. Biol. Chem.* **276,** 28204–28211
47. Sanford, J. L., Edwards, J. D., Mays, T. A., Gong, B., Merriam, A. P., and Rafael-Fortney, J. A. (2005) *J. Mol. Cell. Cardiol.* **38,** 323–332
48. Mays, T. A., Binkley, P. F., Lesinski, A., Doshi, A. A., Quaile, M. P., Margulies, K. B., Janssen, P. M., and Rafael-Fortney, J. A. (2008) *J. Mol. Cell. Cardiol.* **45,** 81–87
49. Irvine, R. F. (2002) *Sci. STKE* **2002,** re13
50. Wilkie, T. M., Scherle, P. A., Strathmann, M. P., Slepak, V. Z., and Simon, M. I. (1991) *Proc. Natl. Acad. Sci. U.S.A.* **88,** 10049–10053
51. Giannone, F., Malpeli, G., Lisi, V., Grasso, S., Shukla, P., Ramarli, D., Sartoris, S., Monsurró, V., Krampera, M., Amato, E., Tridente, G., Colombatti, M., Parenti, M., and Innamorati, G. (2010) *J. Mol. Endocrinol.* **44,** 259–269

J Physiol Sci (2011) 61:167–179
DOI 10.1007/s12576-011-0133-3

ORIGINAL PAPER

DNA microarray profiling identified a new role of growth hormone in vascular remodeling of rat ductus arteriosus

Mei-Hua Jin · Utako Yokoyama · Yoji Sato · Aki Shioda · Qibin Jiao · Yoshihiro Ishikawa · Susumu Minamisawa

Received: 3 December 2010 / Accepted: 28 December 2010 / Published online: 2 February 2011

Abstract The ductus arteriosus (DA), a fetal arterial connection between the pulmonary artery and the aorta, has a character distinct from the adjacent arteries. We compared the transcriptional profiles of the DA and the aorta of Wistar rat fetuses on embryonic day 19 (preterm) and day 21 (near-term) using DNA microarray analyses. We found that 39 genes were expressed 2.5-fold greater in the DA than in the aorta. Growth hormone (GH) receptor (GHR) exhibited the most significant difference in expression. Then, we found that GH significantly promoted migration of DA smooth muscle cells (SMCs), thus enhancing the intimal cushion formation of the DA explants. GH also regulated the expression of cytoskeletal genes in DA SMCs, which may retain a synthetic phenotype in the smooth muscle-specific cytoskeletal genes. Thus, the present study revealed that GH-GHR signal played a role in the vascular remodeling of the DA.

Keywords Growth hormone · Gene expression · Vascular remodeling · Premature infant · Congenital heart disease

Electronic supplementary material The online version of this article (doi:10.1007/s12576-011-0133-3) contains supplementary material, which is available to authorized users.

M.-H. Jin · U. Yokoyama · A. Shioda · Y. Ishikawa (✉) · S. Minamisawa (✉)
Cardiovascular Research Institute, Yokohama City University, 3-9 Fukuura, Kanazawa-ku, Yokohama 236-0004, Japan
e-mail: yishikaw@med.yokohama-cu.ac.jp

S. Minamisawa
e-mail: sminamis@waseda.jp

Y. Sato
Division of Cellular and Gene Therapy Products, National Institute of Health Sciences, 1-18-1 Kamiyoga, Setagaya-ku, Tokyo 158-8501, Japan

Q. Jiao · S. Minamisawa
Department of Life Science and Medical Bioscience, Waseda University Graduate School of Advanced Science and Engineering, 2-2 Wakamatsucho, Shinjuku-ku, Tokyo 162-8480, Japan

Introduction

The ductus arteriosus (DA), a fetal arterial connection between the pulmonary artery and the descending aorta, is essential to fetal life. The morphology and function of the DA dramatically change during development [1]. In particular, during late gestation, the deposition of extracellular matrix in the subendothelium is increased, and the smooth muscle cells (SMCs) of the media migrate into this region, resulting in intimal thickening [2]. This vascular remodeling of the DA is essential for its postnatal closure and is not observed in adjacent arteries. Thus, the DA has distinct characteristic features that differ from those of the adjacent arteries (the aorta and pulmonary arteries). This characteristic of the DA is largely dependent on the expression of the distinct subsets of genes involved in the developmental vascular remodeling that occurs during gestation. To understand the precise transcriptional network in the DA, genome-wide analysis is a powerful approach that can be utilized. In this context, several studies, including ours, have been carried out to identify the effects of oxygen [3] or maternal administration of vitamin A [4] on the transcriptional profiles of the DA. Although the study by Costa et al. [3] is the only one that demonstrated the characteristic differences in the transcriptional profiles between rat DA and the aorta of premature fetuses and neonates, they analyzed their transcriptional profiles on embryonic day 19 (e19) only; they did not examine the changes during later gestation.

Because the morphological and physiological characteristics of the DA differ significantly between premature and mature fetuses [1], it is of great interest to investigate the transcriptional profiles of the DA and the adjacent aorta in the remodeling process that occurs during late gestation.

Materials and methods

Tissue collection for DNA microarray and quantitative reverse transcription polymerase chain reaction analyses

Pooled tissues from the DA or the aorta were obtained from Wistar rat embryos on e19 ($n \geq 120$) and e21 ($n \geq 120$). Reverse transcription polymerase chain reaction (RT-PCR) analysis was performed as described previously [2]. The information on PCR primers for RT-PCR analyses is provided in Supplemental data 1.

Total RNA preparation and DNA microarray analysis

Total RNA preparation and DNA microarray analysis were performed as described previously [4]. Briefly, total RNA was converted to biotin-labeled cRNA that was hybridized to rat genome U34A GeneChip DNA microarray (Affymetrix, Santa Clara, CA). The hybridization experiments were performed in duplicate and the intensities were averaged. If the difference in the signal intensities of a given sequence tag was equal to the cutoff (=2.5-fold) or more, and if the "Comparison Analysis" of the Microarray Suite Software indicated "increased" or "decreased" with the ≥2.5-fold difference at any developmental stage, that sequence tag was considered to exhibit a significant difference between the DA and the aorta.

Primary culture of rat DA SMCs

Vascular SMCs in primary culture were obtained from the DAs of Wistar rat embryos at e21. The tissues were minced and transferred to a 1.5-ml centrifuge tube that contained 800 μl of collagenase-dispase enzyme mixture [1.5 mg/ml collagenase-dispase (Roche), 0.5 mg/ml elastase type II-A (Sigma Immunochemicals, St. Louis, MO), 1 mg/ml trypsin inhibitor type I-S (Sigma), and 2 mg/ml bovine serum albumin fraction V (Sigma) in Hanks' balanced salt solution (Sigma)]. The digestion was carried out at 37°C for 15–20 min. Then cell suspensions were centrifuged, and the medium was changed to the collagenase II enzyme mixture [1 mg/ml collagenase II (Worthington), 0.3 mg/ml trypsin inhibitor type I–S, and 2 mg/ml bovine serum albumin fraction V in Hanks' balanced salt solution]. After 12 min of incubation at 37°C, cell suspensions were transferred to growth medium in 35-mm poly-L-lysine (Sigma)-coated dishes in a moist tissue culture incubator at 37°C in 5% CO_2, 95% ambient mixed air. The growth medium contained Dulbecco's modified Eagle's medium (DMEM) with 10% fetal bovine serum (FBS) and 1% penicillin-streptomycin solution (Sigma). The confluent cells were used at passages 4–6.

SMC migration assay

The migration assay was performed using 24-well Transwell culture inserts with polycarbonate membranes (8-μm pores; Corning Inc.) coated with fibronectin. The DA SMCs were harvested with trypsin-ethylenediamine tetraacetic acid (EDTA), resuspended in serum-free DMEM, and distributed at a density of 1×10^5 cells/100 μl in the inserts. The cells were allowed to settle in serum-free DMEM for 1 h before the addition of GH (20 and 200 ng/ml) in the lower chamber. Under basal conditions, the lower chambers were filled with 600 μl serum-free DMEM. SMCs were then allowed to migrate to the underside of the insert's membrane at 37°C/5% CO_2. At the end of the experiment, the cells were fixed in 10% buffered formalin. SMCs were stained with Cyto Quick (Muto Pure Chemicals), and cells on the upper surface of the membrane were mechanically removed with a cotton swab. Cells that migrated onto the lower surface of the membrane were manually counted from three different fields (0.5 mm^2/field) under a microscope.

Cell proliferation assays

[^{3}H]thymidine incorporation was used to measure cell proliferation in DA SMCs. The SMCs were reseeded into a 24-well culture plate at an initial density of 1×10^5 cells per well for 24 h before serum starvation with DMEM containing 0.1% FBS. Cells were then incubated with or without GH (20 and 200 ng/ml) for 24 h in the starvation medium before addition of 1 μCi of [*methyl*-^{3}H]thymidine (specific activity 5 Ci/mM; Amersham International, Bucks, UK) for 4 h at 37°C. After fixation with 1.0 ml of 10% trichloroacetic acid, the cells were solubilized with 0.5 ml of 0.5 M NaOH and then neutralized with 0.25 ml of 1 N HCl. A liquid scintillation counter was used to measure [^{3}H]thymidine incorporation. Data obtained from triplicate wells were averaged.

Quantitation of hyaluronan

The amount of hyaluronan in the cell culture supernatant was measured by a latex agglutination method based on the specific interaction of hyaluronan with the latex-labeled hyaluronan-binding protein from bovine cartilage (Fujirebio Inc.). Hyaluronan was quantified in duplicate according to

the manufacturer's instructions using 2.5-μl aliquots of the conditioned cell culture medium using the HITACHI 7070 analysis system (Hitachi) at an 800-nm wavelength.

Organ culture

Fetal arteries including the DA and the aortic arch arteries were incubated with GH (200 ng/ml) for 72 h in serum-free DMEM as described previously [2]. Explants were then fixed in 10% buffered formalin and embedded in paraffin. The sectioned segments in the middle portion of the DA were analyzed histochemically.

Immunohistochemistry

Tissue staining and immunohistochemistry were performed as described previously [5, 6]. Mouse monoclonal anti-GHR antibody (MAB263) was purchased from Abcam (Tokyo, Japan).

Statistics

Data are presented as mean ± standard error (SEM) of independent experiments. Statistical analysis was performed between two groups by unpaired two-tailed Student's *t* test or unpaired *t* test with Welch correction, and among multiple groups by one-way analysis of variance (ANOVA) followed by Neuman-Keuls multiple comparison test. A p value of <0.05 was considered significant.

Results

Genes differentially expressed between the DA and the aorta

All the microarray data in the present study were deposited at the Gene Expression Omnibus (GEO) repository (http://www.ncbi.nlm.nih.gov/projects/geo/; accession no. GSE3422). A total of 117 genes (142 probe sets) showed a significant difference (≥2.5-fold) between the DA and the aorta at e19 or e21. Among 117 genes, 39 (43 probe sets) exhibited a DA-dominant expression pattern (Table 1), and 78 (99 probe sets) exhibited an aorta-dominant expression pattern (Table 2).

Of 39 genes in the DA-dominant expression pattern (Table 1), 34 had a known function, and 3 were homologous to known genes. Although several genes, such as prostaglandin E receptor 4 (subtype EP4) (Ptger4) and endothelin-1, are known to play an important role in the regulation of vascular tone of the DA [1], the role of most of the other genes in the DA has not been identified. We found that growth hormone (GH) receptor exhibited the highest difference in the expression between the DA and the aorta among 39 DA-dominant genes.

Of the 39 genes, 9 encode proteins related to cytoskeleton and the extracellular matrix, including sarcomeric genes such as Myh11 (myosin heavy chain 11), Myl6 (myosin light chain, polypeptide 6, alkali, smooth muscle and non-muscle), Actg2 (actin, gamma 2), Tpm1 (tropomyosin 1, alpha), Tnn (tenascin N, predicted), and Lamb2 (laminin beta2). Three membrane ion channels, ATPase Na^+/K^+ transporting b1 polypeptide and potassium inwardly rectifying channel (Atp1b1), subfamily J, member 8 (Kcnj8), which is known as ATP-sensitive potassium channel K_{ATP}-1, and Ca^{2+} channel, voltage-dependent, $\alpha 2/\delta$ subunit 1 (Cacna2d1), were also strongly expressed in the DA.

We also identified 79 genes in the aorta-dominant expression pattern (Table 2). Of the 79 genes, 14 genes encode proteins related to cytoskeleton and the extracellular matrix. Cardiac sarcomeric genes such as Myh6 (myosin heavy chain, polypeptide 6), Myh7 (myosin heavy chain, polypeptide 7), Myl7 (myosin, light polypeptide 7, regulatory), Myl2 (myosin regulatory light chain 2, ventricular/cardiac muscle isoform), Actc1 (alpha, actin alpha cardiac 1), Tnnt2 (troponin T2, cardiac), Tnni3 (troponin I, cardiac), and Fn1 (fibronectin 1) were more highly expressed in the aorta than in the DA. Accordingly, there was a marked difference in the composition of the genes related to the cytoskeleton and the extracellular matrix between the DA and the aorta. Sixteen genes were expressed 2.5-fold more in the aorta at both e19 and e21 than in the DA, whereas 24 genes were expressed 2.5-fold more in the aorta than in the DA only at e21. To confirm the results of the DNA microarray, we performed RT-PCR (Supplemental data 2).

Growth hormone receptor mRNA and protein were dominantly expressed in the developing DA

As mentioned above, GH receptor (GHR) exhibited the highest difference of expression between the DA and the aorta (Fig. 1a), suggesting that GH-GHR signal plays a distinct role in the vascular remodeling of the DA from the aorta. The expression of GH mRNA was very low, and there was no difference between the DA and the aorta (Fig. 1b). Interestingly, the expression levels of insulin-like growth factor (IGF)-I and IGF-II mRNAs were higher in the aorta than in the DA, whereas the expression levels of IGF-I receptor (IGF-IR) and IGF-IIR mRNAs did not differ (Fig. 1c–f). In addition, the expression levels of IGF binding protein (IGFBP) 2 and IGFBP5 mRNAs were also higher in the aorta than in the DA at e21 and at e19, respectively (Table 2).

The expression of GHR mRNA was also confirmed by quantitative RT-PCR analyses. We found that the expression levels of GHR mRNA were higher in the rat DA than

Table 1 DA-dominant genes

	Probe set ID	RefSeq Transcript ID	Gene title	Gene symbol	Fold difference between DA and aorta	
					e19	e21
1	**rc_AI104225_at**	**NM_017094**	**Growth hormone receptor**	**Ghr**	**5.0**	**8.7**
2	Z83757mRNA_at	XM_222794	Tenascin N (predicted)	Tnn_predicted	2.3	7.4
3	L16764_s_at/// Z75029_s_at	NM_031971/// NM_212504	Heat shock 70kD protein 1A///heat shock 70kD protein 1B	Hspa1a///Hspa1b	8.6	7.1
4	rc_AA891527_at	NM_022531	Desmin	Des	1.4	6.3
5	rc_AA893846_at	NM_053591	Dipeptidase 1 (renal)	Dpep1	3.4	5.6
6	X73524_at	NM_013129	Interleukin 15	Il15	2.0	5.6
7	D28561_s_at	NM_031677	Four and a half LIM domains 2	Fhl2	3.4	4.9
8	rc_AA894200_at	XM_342032	Proprotein convertase subtilisin/kexin type 5	Pcsk5	1.4	4.8
9	AF002281_at	NM_012870	Tumor necrosis factor receptor superfamily, member 11b (osteoprotegerin)	Tnfrsf11b	1.2	4.7
10	M22323_at	NM_013086/// NM_017334	cAMP responsive element modulator	Crem	1.8	3.5
11	U94330_at	NM_001007678	Mss4 protein	Mss4	1.5	3.1
12	rc_AA799773_at	NM_134410	Mg87 protein	Mg87	1.3	2.9
13	X82152_at	NM_001002287	MAS-related G protein-coupled receptor, member B4	Mrgprb4	2.5	2.9
14	M64711_at	NM_080698	Fibromodulin	Fmod	1.6	2.8
15	D28860_s_at	NM_012893	Actin, gamma 2	Actg2	3.7	2.8
16	U69272_g_at	NM_017099	Potassium inwardly rectifying channel, subfamily J, member 8	Kcnj8	2.8	2.8
17	rc_AA859578_at	NM_021587	Latent transforming growth factor beta binding protein 1	Ltbp1	2.0	2.7
18	rc_AA859954_at	NM_012751	Solute carrier family 2 (facilitated glucose transporter), member 4	Slc2a4	2.3	2.7
19	rc_AI014135_g_at	NM_013113	ATPase, Na +/K + transporting, beta 1 polypeptide	Atp1b1	2.1	2.7
20	rc_AI176662_s_at	NM_019131	Tropomyosin 1, alpha	Tpm1	2.3	2.7
21	AB020504_g_at	NM_032076	Prostaglandin E receptor 4 (subtype EP4)	Ptger4	2.4	2.6
22	rc_AI232078_at	NM_012827	Bone morphogenetic protein 4	Bmp4	2.8	2.6
23	U02553cds_s_at	NM_033485	PRKC, apoptosis, WT1, regulator	Pawr	1.4	2.6
24	X63253cds_s_at	NM_080902	Hypoxia induced gene 1	Hig1	1.7	2.6
25	M60921_g_at	XR_086177	PMF32 protein (predicted)	Pmf31	2.8	2.5
26	S66024_at	XM_343144	Myosin, light polypeptide 6, alkali, smooth muscle and non-muscle (predicted)	Myl6_predicted	2.7	2.5
27	M86621_at	NM_012887	Thymopoietin	Tmpo	1.2	2.5
28	X54686cds_at/// rc_AA891041_at	XM_573030	Myosin heavy chain 11	Myh11	3.7	2.3
29	U17254_g_at	NM_012974	Laminin, beta 2	Lamb2	2.5	2.3
30	Z22607_at	NM_019620	Zinc finger protein 386 (Kruppel-like)	Znf386	7.5	2.2
31	rc_AA891422_at	NM_053650	PDZ and LIM domain 3	Pdlim3	2.6	1.8
32	rc_AI144767_s_at/// rc_AA875132_at	NM_024162	Fatty acid binding protein 3	Fabp3	3.5	1.7
33	M63656_s_at	NM_012919	Calcium channel, voltage-dependent, alpha2/delta subunit 1	Cacna2d1	2.7	1.6
34	rc_AI014163_at	NM_012548	Endothelin 1	Edn1	2.8	1.4
35	rc_AI639161_at	XM_346029	Similar to KIAA1411 protein (predicted)	RGD1304927_predicted	2.7	1.2
36	rc_AA866345_at	NM_012531	Catechol-*O*-methyltransferase	Comt	4.6	1.2
37	rc_AI230614_s_at/// rc_AI112173_at	NM_001002829	RAS-like family 11 member A	Rasl11a	3.0	1.1
38	rc_AA799511_g_at	–	–	–	1.8	2.6
39	rc_AA893871_at	–	–	–	1.4	2.5

Table 2 Aorta-dominant genes

	Probe set ID	RefSeq transcript ID	Gene title	Gene symbol	Fold difference between aorta and DA	
					e19	e21
1	X15939_r_at///rc_AI104924_f_at/// rc_AI103920_f_at///rc_AA891522_f_at	NM_017239	Myosin heavy chain, polypeptide 6, cardiac muscle, alpha	Myh6	2.2	23.8
2	X80130cds_i_at///rc_AI104567_g_at/// rc_AA866452_s_at	XM_215801	Actin alpha cardiac 1	Actc1	3.0	18.4
3	M93638_at	NM_183333	Keratin complex 2, basic, gene 5	Krt2-5	6.9	16.8
4	rc_AA891242_g_at///rc_AA891242_at	NM_001106017	Myosin, light polypeptide 7, regulatory	Myl7	3.2	15.3
5	X15939_f_at	NM_017240	Myosin, heavy polypeptide 7, cardiac muscle, beta	Myh7	1.9	13.2
6	D78159mRNA_s_at	NM_001008806	Type II keratin Kb4	Kb4	1.5	9.1
7	X15512_at	NM_012824	Apolipoprotein C–I	Apoc1	0.5	7.4
8	U67914_at	XM_342219	Carboxypeptidase A3	Cpa3	1.7	7.2
9	rc_AI169372_g_at	NM_031839	Cytochrome P450, family 2, subfamily c, polypeptide 23	Cyp2c23	0.5	5.5
10	K01933_at	NM_012582	Haptoglobin	Hp	0.5	5.1
11	M80829_at	NM_012676	Troponin T2, cardiac	Tnnt2	1.3	4.8
12	X00975_g_at///X07314cds_at	NM_001035252	Myosin, light polypeptide 2	Myl2	5.1	4.8
13	M24852_at	NM_013002	Purkinje cell protein 4	Pcp4	4.7	4.8
14	M92074_g_at	NM_017144	Troponin I, cardiac	Tnni3	2.1	4.6
15	rc_AA945054_s_at	NM_022245	Cytochrome b-5	Cyb5	0.8	4.1
16	S76779_s_at	NM_138828	Apolipoprotein E	Apoe	1.3	3.9
17	AF014503_at	NM_053611	Nuclear protein 1	Nupr1	3.2	3.9
18	X02412_at	NM_019131	Tropomyosin 1, alpha	Tpm1	1.0	3.7
19	D00752_at	NM_182474	Serine protease inhibitor	Spin2a	0.5	3.6
20	D89730_at	NM_001012039	Epidermal growth factor-containing fibulin-like extracellular matrix protein 1 (predicted)	Efemp1_predicted	4.0	3.6
21	M14656_at	NM_012881	Secreted phosphoprotein 1	Spp1	4.7	3.4
22	X81448cds_at///rc_AI072634_at	NM_053976	Keratin complex 1, acidic, gene 18	Krt1-18	1.5	3.1
23	rc_AA946368_at	XM_575338	Similar to fatty acid translocase/CD36	LOC499984	1.9	3.1
24	M91595exon_s_at///J04486_at/// A09811cds_s_at	NM_013122	Insulin-like growth factor binding protein 2	Igfbp2	2.1	3.1
25	U30938_at	NM_013066	Microtubule-associated protein 2	Mtap2	2.1	3.0
26	Y12502cds_at	NM_021698	Coagulation factor XIII, A1 subunit	F13a	2.8	2.9
27	M84719_at	NM_012792	Flavin containing monooxygenase 1	Fmo1	4.4	2.8
28	M91652complete_seq_at	NM_017073	Glutamine synthetase 1	Glul	1.8	2.8
29	J03752_at	NM_134349	Microsomal glutathione *S*-transferase 1	Mgst1	1.1	2.7
30	AF072411_g_at///rc_AA925752_at	NM_031561/// XM_575338/// XM_575339	CD36 antigen///similar to fatty acid translocase/CD36///similar to fatty acid translocase/CD36	Cd36///LOC499984/// LOC499985	1.7	2.7
31	L19998_g_at///L19998_at	NM_031834	Sulfotransferase family 1A, phenol-preferring, member 1	Sult1a1	2.9	2.7
32	L25387_g_at	NM_206847	Phosphofructokinase, platelet	Pfkp	1.7	2.6
33	rc_AI230247_s_at	NM_019192	Selenoprotein P, plasma, 1	Sepp1	2.2	2.6
34	rc_AI237731_s_at///L03294_g_at///L03294_at	NM_012598	Lipoprotein lipase	Lpl	0.9	2.6
35	M83680_at	NM_053589	RAB14, member RAS oncogene family	Rab14	2.6	2.6
36	rc_AI639532_at	XM_215935	Troponin C2, fast (predicted)	Tnnc2_predicted	4.7	2.5
37	X71127_g_at	NM_019262	Complement component 1, q subcomponent, beta polypeptide	C1qb	3.2	2.5
38	AB000113_at	NM_017217	Solute carrier family 7 (cationic amino acid transporter, y + system), member 3	Slc7a3	1.6	2.5
39	rc_AA894092_at	XM_342245	Periostin, osteoblast specific factor (predicted)	Postn_predicted	2.5	2.5
40	M32062_g_at	NM_053843/// XM_573502/// XM_573503	Fc receptor, IgG, low affinity III///Fc gamma receptor II beta///similar to low affinity immunoglobulin gamma Fc region receptor III precursor (IgG Fc receptor III) (Fc-gamma RIII) (FcRIII)	Fcgr3/// LOC498276/// LOC498277	3.2	2.4
41	M24353_g_at	XM_343636	Mannosidase 2, alpha 1	Man2a1	4.7	2.3

Table 2 continued

	Probe set ID	RefSeq transcript ID	Gene title	Gene symbol	Fold difference between aorta and DA	
					e19	e21
42	U77931_at	NM_147136	rRNA promoter binding protein	RGD:727924	3.0	2.3
43	M12098_s_at	NM_012604	Myosin, heavy polypeptide 3, skeletal muscle, embryonic	Myh3	2.7	2.1
44	AJ005396_at	XM_342325	Procollagen, type XI, alpha 1	Col11a1	3.1	2.1
45	rc_AA893230_at	XM_236325	Ceroid-lipofuscinosis, neuronal 6 (predicted)	Cln6_predicted	2.8	2.1
46	rc_AA875172_at	NM_053360	SH3-domain kinase binding protein 1	Sh3kbp1	2.6	2.1
47	AB012235_at///AB012234_g_at/// AB012234_at	XM_213849	Nuclear factor I/X	Nfix	4.9	1.9
48	X00722_at	XM_578812	Similar to testin	LOC503278	2.8	1.9
49	M32062_at	NM_053843/// XM_573502	Fc receptor, IgG, low affinity III///Fc gamma receptor II beta	Fcgr3///LOC498276	2.8	1.8
50	rc_AI013472_at///rc_AA924925_at	NM_138905	ER transmembrane protein Dri 42	Ppap2b	2.6	1.8
51	U62897_at	NM_012836	Carboxypeptidase D	Cpd	3.0	1.8
52	Z12298cds_s_at///X59859_r_at///X59859_i_at	NM_024129	Decorin	Dcn	2.7	1.7
53	M15797_at	XM_213954	Nidogen (entactin)	Nid	13.4	1.7
54	AF041066_at	NM_020082	Ribonuclease, RNase A family 4	Rnase4	2.9	1.7
55	U50842_at	XM_343427	Neural precursor cell expressed, developmentally downregulated gene 4A	Nedd4a	3.9	1.6
56	rc_AA866443_at	NM_001008560	Protease, serine, 35 (predicted)	Prss35	4.2	1.6
57	S66184_s_at///rc_AI234060_s_at/// rc_AI102814_at///rc_AA875582_at	NM_017061	Lysyl oxidase	Lox	3.2	1.6
58	rc_AI639314_at	XM_238213	Delangin (predicted)	NIPBL_predicted	2.5	1.6
59	rc_AA800908_at	XM_344450	Potassium channel tetramerisation domain containing 12 (predicted)	Kctd12_predicted	3.6	1.6
60	rc_AI029920_s_at	NM_012817	Insulin-like growth factor binding protein 5	Igfbp5	4.0	1.5
61	L10326_at	NM_019132	GNAS complex locus	Gnas	2.7	1.5
62	E00988mRNA_s_at	NM_031511	Insulin-like growth factor 2	Igf2	3.0	1.4
63	U01908cds_s_at///D43778exon#3_s_at/// D16840_s_at	NM_012494	Angiotensin II receptor, type 2	Agtr2	4.4	1.4
64	rc_AI176461_s_at	NM_017211	Golgi apparatus protein 1	Glg1	3.3	1.4
65	U23146cds_s_at	NM_057103	A kinase (PRKA) anchor protein (gravin) 12	Akap12	2.9	1.4
66	rc_AA900750_s_at	NM_012760	Pleiomorphic adenoma gene-like 1	Plagl1	2.5	1.4
67	Z17223_at	NM_017149	Mesenchyme homeo box 2	Meox2	2.6	1.3
68	rc_AI171966_at	NM_198740	Major histocompatibility complex, class II, DM beta	RGD:735096	2.5	1.2
69	U35775_g_at///U35775_at	NM_031552	Adducin 3 (gamma)	Add3	5.3	1.2
70	U43534_at	NM_012894	Adenosine deaminase, RNA-specific, B1	Adarb1	2.7	0.8
71	AF004811_at	NM_030863	Moesin	Msn	2.9	0.7
72	X05831cds_at///U82612cds_at///M28259cds_at	NM_019143	Fibronectin 1	Fn1	3.9	0.7
73	U17604_at	NM_053865	Reticulon 1	Rtn1	2.6	0.7
74	X51531cds_g_at///X51531cds_at	–	–	–	4.4	30.2
75	rc_AA799865_at	–	Transcribed locus	–	1.3	2.7
76	X05472cds#2_at	–	–	–	7.2	2.4
77	rc_AA799406_at	XM_578859	Hypothetical protein LOC503325	LOC503325	2.6	1.3
78	rc_AA859921_at	–	–	–	3.3	0.9

in the aorta at e19 and at e21 ($p < 0.05$ and $p < 0.001$, $n = 6$–8, respectively) (Fig. 2a).

We then examined the localization of GHR in the DA and the aorta at e19 and e21. GHR immunoreactivity was detected abundantly in the SMC layer and less in the endothelial cells of the DA (Fig. 2b).

GH promoted DA SMC migration, but not proliferation

SMC migration and proliferation play an essential role in intimal cushion formation of the DA, especially during late gestation. Therefore, we investigated the effects of GH on migration and proliferation using DA SMCs in primary

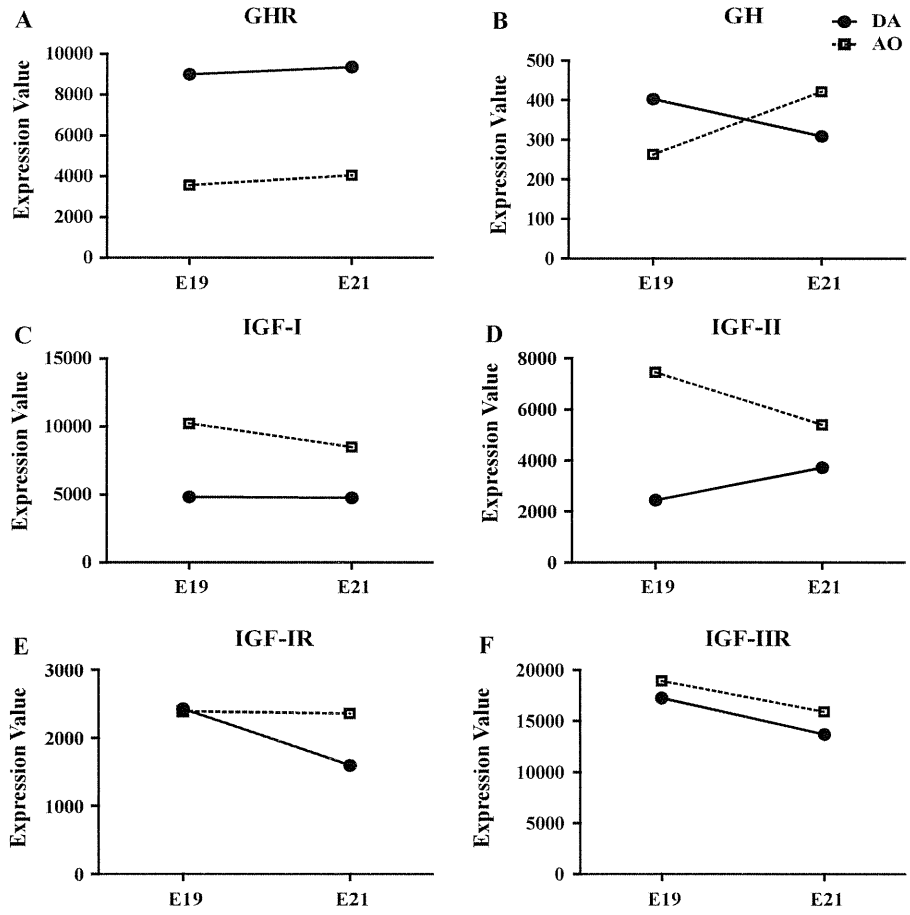

Fig. 1 The expression of growth hormone receptor and its related genes in the developing DA by DNA microarray analysis. **a** GHR (growth hormone receptor), **b** GH (growth hormone), **c** IGF (insulin-like growth factor)-I, **d** IGF-II, **e** IGF-IR (type I receptor), and **f** IGF-IIR (type II receptor) mRNA. *E19* Embryonic day 19, *E21* embryonic day 21, *DA* ductus arteriosus, *AO* aorta

culture from rat DA at e21. We found that recombinant rat GH promoted migration of DA SMCs in a dose-dependent manner (Fig. 3a). However, the same amount of GH did not promote migration of aortic SMCs (Supplemental data 3). When DA SMCs were treated with platelet-derived growth factor BB (PDGF-BB) (10 ng/ml), a potent stimulator for SMC migration, SMC migration was significantly increased by 141% in DA SMCs. In contrast, [^{3}H]thymidine incorporation was unchanged in DA SMCs in the presence of recombinant rat GH (up to 200 ng/ml) (Fig. 3b). When DA SMCs were treated with 10% FBS, a potent stimulator for SMC proliferation, [^{3}H]thymidine incorporation was significantly increased by 112% in DA SMCs. Hyaluronan is an important component of the intimal cushion, and hyaluronan-rich matrices are essential for cell migration and proliferation in the DA [2]. Because our recent study revealed that PGE_1 is a potent stimulator for hyaluronan production in DA SMCs [2], we investigated whether or not GH altered hyaluronan production in DA SMCs. We found that GH had no effect on hyaluronan production in DA SMCs (data not shown).

Effect of GH on tissue-specific cytoskeletal genes in the DA and the aorta

Our DNA array analyses revealed that the expression of cytoskeletal genes was markedly different between the DA and the aorta. Because GH is known to regulate cytoskeletal organization [7], we examined whether or not GH affected such a tissue-specific expression of cytoskeletal genes in DA SMCs. We found that GH decreased the expression of DA-dominant cytoskeletal genes such as desmin, Fhl2, Actg2, and Myh11 in DA SMCs (Fig. 4a–d). Among the aorta-dominant sarcomere genes, we also found that GH decreased the expression of Myl2 and Tnnt2 mRNAs, increased the expression of Tnni3 mRNA, and exhibited no change in Myh7, Actc1, and Tnnc2 mRNAs (Fig. 5).

Because GH is known to inhibit the expression of skeletal muscle-specific proteins in a dose-dependent manner in satellite cells [8], we examined the effect of GH on the expression of smooth muscle-specific genes. We found that GH significantly decreased the expression of SM1, SM2, SM22, and h-caldesmon mRNAs, whereas GH did not

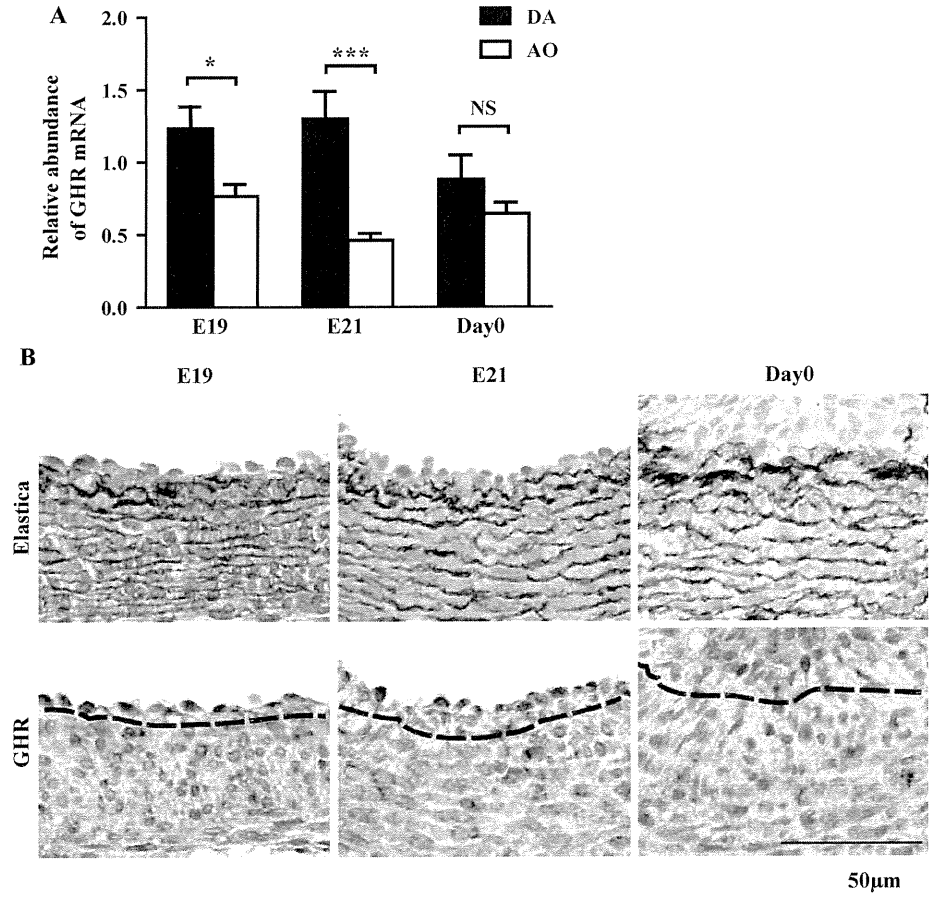

Fig. 2 Expression of GHR mRNA and protein in rat DA. **a** Quantitative RT-PCR analyses of GHR. The expression level of GHR mRNA was maximal at E19 and E21 in the DA ($n = 6$–8). **b** Immunohistological analysis of GHR protein in the rat DA at E19, E21, and Day0. GHR was detected in a *brown color*. Dark blue stain was counterstained with Mayer's hematoxylin. *Scale bars* 50 mm. $*p < 0.05$, $***p < 0.001$. Data are expressed as means ± SEM. *E19* Embryonic day 19, *E21* embryonic day 21, *Day0* at birth, *DA* ductus arteriosus, *AO* aorta, *GHR* growth hormone receptor, *NS* not significant

change the expression of SMemb mRNA (Fig. 6a–e). We also found that GH decreased the expression of myocardin mRNA (Fig. 6f), a transcriptional factor, which is sufficient for a smooth muscle-like contractile phenotype. To investigate whether the effect of GH on the expression of cytoskeletal genes is found in aortic SMCs, we also did the same experiment using SMCs from the rat aorta at e21. We also found a similar effect of GH on the expression of cytoskeletal genes in cultured rat aortic SMCs (Supplemental data 4, 5, and 6).

GH promoted intimal thickening of immature rat DA explants

To examine to what extent GH contributes to the intimal thickening of the DA, we administrated GH into the premature vessel explants containing the DA, the aorta, and the main pulmonary artery from fetuses at e19 (Fig. 7). We found that GH significantly promoted intimal thickening of the DA, but not the aorta when compared with the control (Fig. 7). It should be noted that the effect of GH on the intimal thickening was greater in the DA than in the aorta.

Discussion

Our microarray analyses uncovered gene expression profiles of the DA distinct from those of the aorta during fetal development. These gene expression profiles are considered to be the primary determinant of the different functional and morphological characteristics of the DA from the adjacent arteries. In fact, several unexpected genes that are known to be involved in tissue differentiation were identified as having a DA-dominant expression pattern. It is of note that among them GHR exhibited the highest difference in expression between the rat developing DA and the adjacent aorta. Although the expression levels of GH mRNA were slightly higher in the aorta than in the DA at e21, the difference did not reach statistical significance. We think that total GH-GHR signals are higher in the DA than in the aorta due to the predominant expression of GHR in the DA during gestation. Accordingly, we hypothesized that GH stimulation via GHR may be involved in DA remodeling and that it may play a role in the specification of the DA from other arteries. During gestation, the serum GH concentration of fetuses increased gradually as

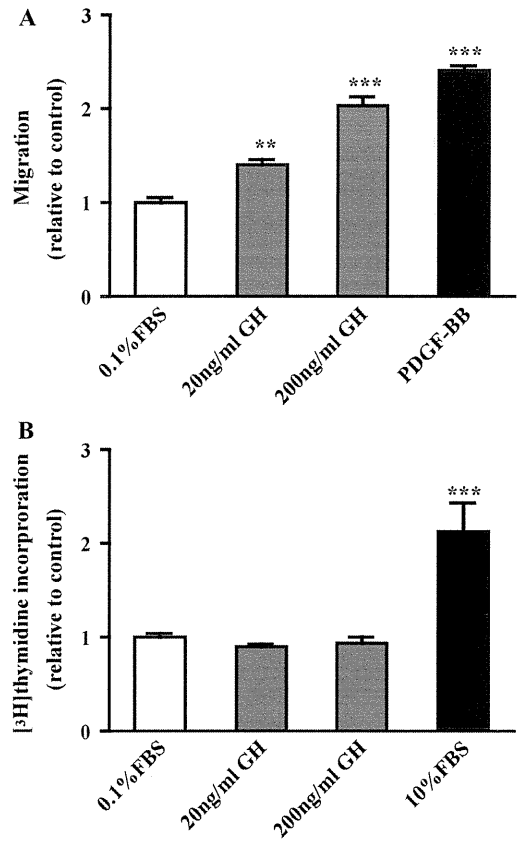

Fig. 3 GH promoted DA SMC migration, but not proliferation. **a** Effects of growth hormone (GH) stimulation on DA SMC migration. DA SMC migration was significantly increased in the presence of GH at a concentration of 20 or 200 ng/ml ($n = 6$). PDGF-BB at a concentration of 10 ng/ml was used as a positive control. **b** The effect of GH on proliferation of rat DA SMCs. GH did not promote cell proliferation in DA SMCs ($n = 6$–8); 10% FBS was used as a positive control. $^{**}p < 0.01$,$^{***}p < 0.001$ versus 0.1% FBS. Data are expressed as means ± SEM. *FBS* Fetal bovine serum

pregnancy advanced and declined before parturition in many species [9–11]. In rodents, the fetal pituitary gland starts to secret GH from e15, whereas many tissues, including vascular endothelial and SMCs, locally produce GH beginning in relatively early embryogenesis [12]. Even though the level of serum GH in a fetus is almost comparable to or slightly less than that in an adolescenct [9–11], GH has been regarded as of little functional significance in fetal growth [13]. A growing body of evidence, however, has revealed the importance of GH in tissue differentiation during fetal development. First, many fetal tissues, including vascular endothelium and smooth muscle, express GHR [14, 15]. Therefore, GH likely activates an intracellular signal pathway through GHR in fetuses. Second, a considerable number of studies have demonstrated that fetal tissues indeed respond to GH in vitro [12, 16], which was observed in the present study. Third, GHR knockout mice exhibit functional and morphological changes in both heart and vasculature [17]. These results led us to explore the role of GH in DA development, especially in its vascular remodeling.

Numerous previous studies have demonstrated that GH plays a role in angiogenesis [18] and that GH deficiency or excess increases the risk of cardiovascular morbidity and mortality [19, 20]. However, the role of GH in the vascular remodeling of the developmental arteries has not yet been precisely evaluated. The present study revealed that GH promoted the migration of DA SMCs and then intimal cushion formation in DA explants. In terms of the effect of GH on SMC migration, data from previous studies are very limited [21–23]. Although the precise mechanism still has not been investigated, it can be assumed that the different responses to GH in various cell types are dependent on the GHR expression levels.

Intimal thickness is a hallmark of physiological vascular remodeling of the DA during late gestation [2]. Although the present study demonstrated that GH promotes intimal cushion formation of the ex vivo DA explants, previous clinical studies have shown that the effect of GH on pathological intimal thickness is equivocal. Increases in the carotid intimal media thickness were observed in patients with acromegaly [24]. In contrast, patients with either childhood- or adulthood-onset GH deficiency also exhibited increased intima-media thickness and endothelial dysfunction [19, 25]. Therefore, adequate levels of GH could be important to maintain normal morphology of mature arteries. The present study indicates that GH in the culture media at a concentration of 200 ng/ml is sufficient to promote the physiological intimal cushion formation of the DA through increasing SMC migration.

It is known that the differentiation of DA SMCs precedes that of other arteries [26, 27]. Nevertheless, we were surprised by the considerable number of cardiac-type sarcomere genes expressed in the fetal DA, although it was much less than that in the aorta. The present data suggest that prior to complete differentiation, vascular SMCs may retain a high degree of plasticity, which allows them to modulate their phenotype [28]. Interestingly, through the in vitro experiment, we found that the effect of GH on the expression of the cytoskeletal genes was not always consistent with the tissue-dominant expression patterns that were identified by DNA microarray analysis. Therefore, factor(s) other than GH may determine the tissue-specific expression pattern of cytoskeletal genes in the DA and the aorta.

More importantly, we found that GH downregulated the genes involved in a smooth muscle-like contractile phenotype. Consistent with the result, we also found that GH downregulated myocardin mRNA, which is sufficient for a smooth muscle-like contractile phenotype [28]. In addition

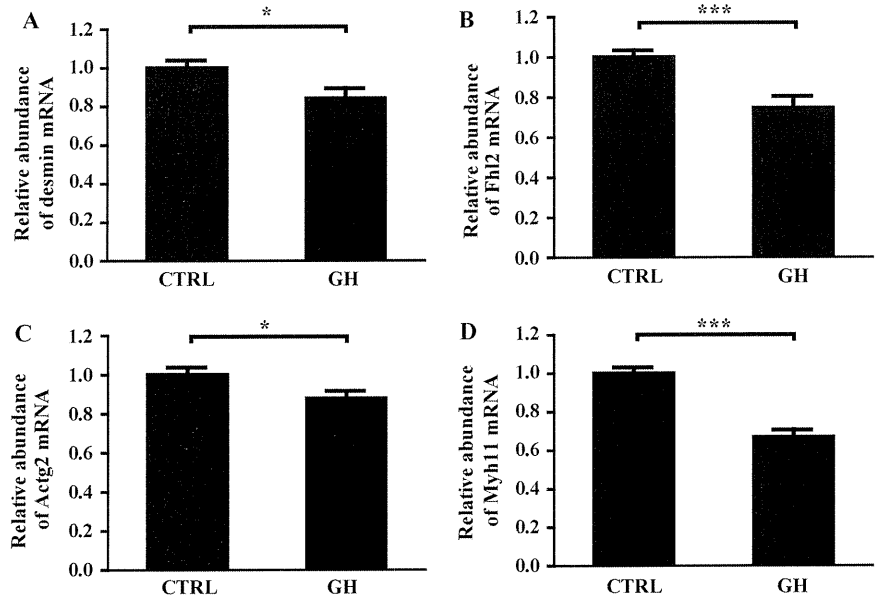

Fig. 4 Effect of GH on the cytoskeletal genes and smooth muscle-specific genes in DA SMCs. **a** Desmin, **b** Fhl2, **c** Actg2, **d** Myh11. ($n = 15$). $*p < 0.05$, $***p < 0.001$. Data are expressed as means ± SEM. *GH* Growth hormone, *CTRL* control, *DA SMC* ductus arteriosus smooth muscle cell, *NS* not significant

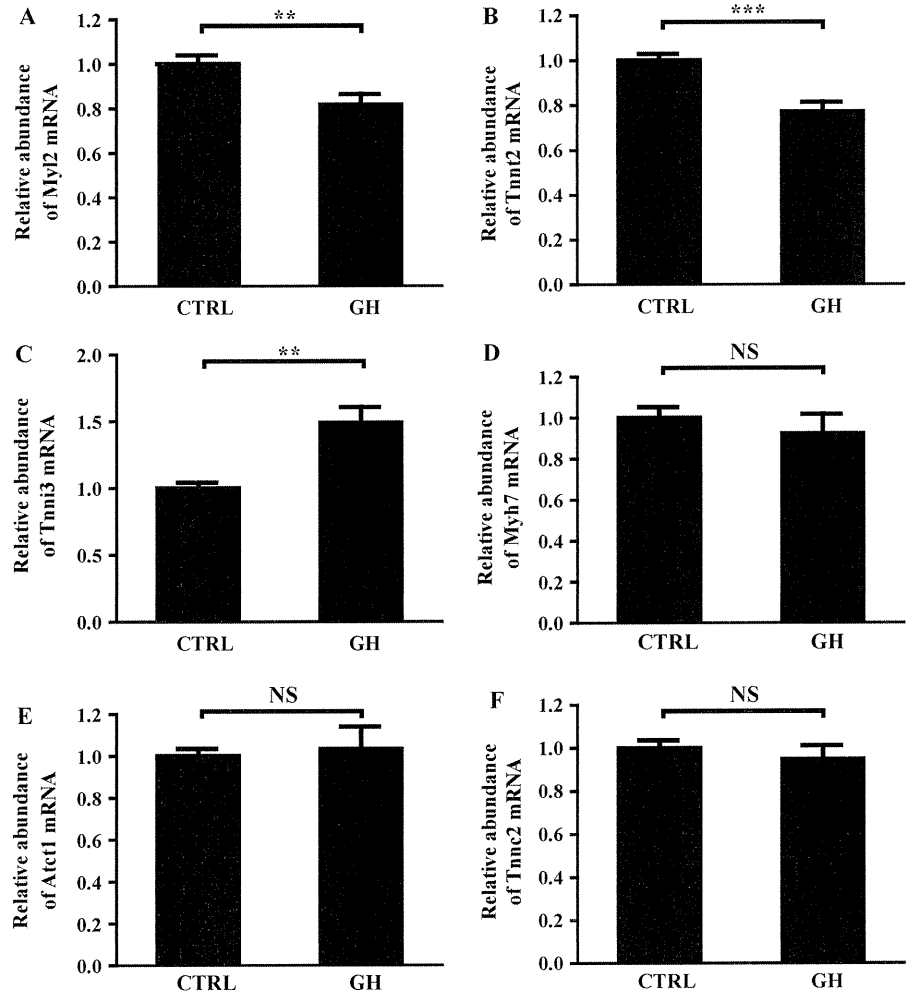

Fig. 5 Effect of GH on the expression of the aorta-dominant sarcomere genes in DA SMCs. **a** Myl2, **b** Tnnt2, **c** Tnni3, **d** Myh7, **e** Actc1, and **f** Tnnc2. ($n = 15$). $**p < 0.01$, $***p < 0.001$. Data are expressed as means ± SEM. *GH* Growth hormone, *CTRL* control, *DA SMC* ductus arteriosus smooth muscle cell, *NS* not significant

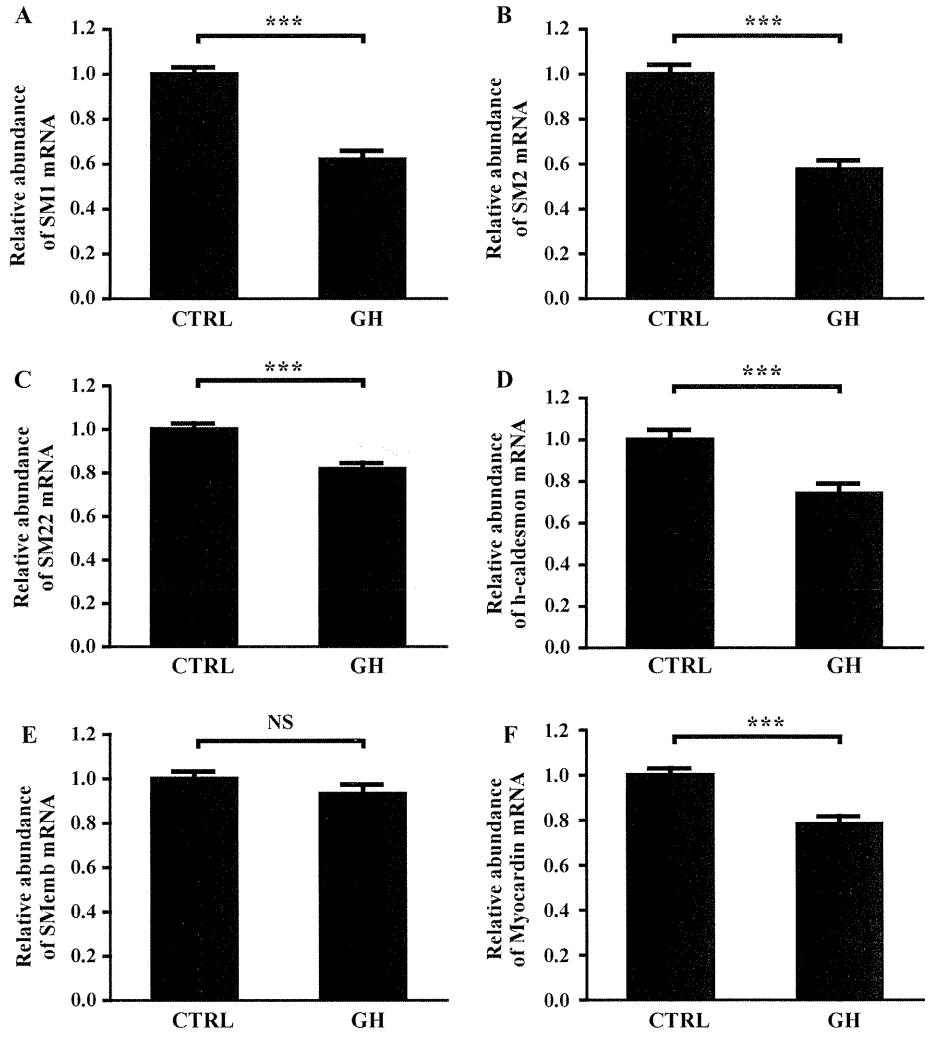

Fig. 6 Effect of GH on the cytoskeletal genes and smooth muscle-specific genes in DA SMCs. **a** SM1, **b** SM2, **c** SM22, **d** h-caldesmon, **e** SMemb, **f** Myocardin. ($n = 15$). $*p < 0.05$, $***p < 0.001$. Data are expressed as means ± SEM. *GH* Growth hormone, *CTRL* control, *DA SMC* ductus arteriosus smooth muscle cell, *NS* not significant

to this observation, Halevy et al. [8] demonstrated that GH inhibited the gene expression of myogenin and the expression of skeletal muscle-specific proteins in a dose-dependent manner in satellite cells. These data suggested that during muscle differentiation, GH inhibited the muscle-specific differentiation at its final stage to retain its synthetic phenotype. We propose that DA SMCs consist of distinct types that depend on their localization. During the progression of intimal cushion formation, DA SMCs in the inner layer are a synthetic phenotype that is highly proliferative and can migrate easily. The GH-GHR signal helps these cells remain a synthetic phenotype. Further studies are required to prove this idea.

Although the present microarray analyses uncovered distinct gene expression profiles of the DA from those of the aorta, several gene profiles are different from a previous report demonstrating the transcriptional profiles between the rat DA and the aorta of premature fetuses and neonates using the same DNA microarray plates we used [3]. For example, Costa et al. demonstrated that Myl2 and Myh7 are predominantly expressed in the rat aorta at e19, but our data showed the opposite result. In addition, the tissue-specific genes that we identified overlap very little with their findings. We do not have a reasonable explanation for this discrepancy. It should be noted that the present study identified several expected genes that are known to be predominantly expressed in the DA, such as prostaglandin E receptor 4, endothelin-1, and Kcnj8 (potassium inwardly rectifying channel, subfamily J, member 8). In contrast, Costa et al. did not identify this expected DA-dominant gene in the data from their microarray analysis. Furthermore, we also confirmed by quantitative RT-PCR analysis that, using different sets of RNA samples, the expression of several DA-dominant genes was higher in the DA than in the aorta. Therefore, we are confident that we provided

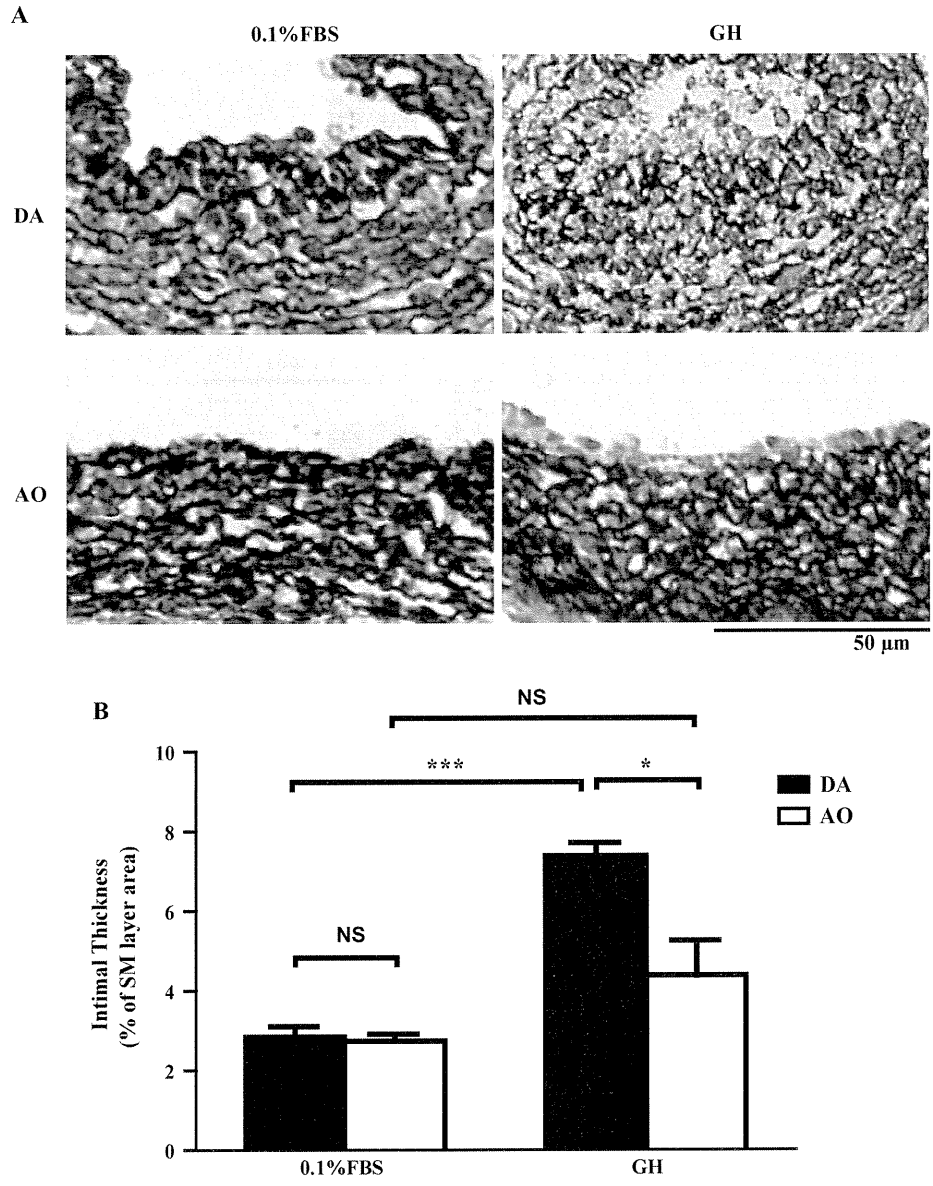

Fig. 7 Effects of GH-mediated intimal thickening of immature rat DA and aorta explants. **a** Elastica staining of the DA and the aorta. GH at a concentration of 200 ng/ml. *Scale bars* 50 μm. **b** GH significantly promoted intimal thickening of the DA, but not the aorta. ($n = 4$–6). $^{*}p < 0.05$,$^{***}p < 0.001$. Data are expressed as means ± SEM. *DA* Ductus arteriosus, *AO* aorta, *GH* growth hormone, *NS* not significant

reliable data regarding the transcriptional profiles of the developing rat DA.

In conclusion, our study highlighted the distinct transcriptional profiles of the DA. In addition to the expected genes, microarray analysis revealed many genes whose roles were previously unrecognized in the DA. Among them, we found that the GH-GHR signal plays a role in vascular remodeling of the DA by promoting migration of SMCs and the subsequent formation of intimal thickness and regulating the expression of cytoskeletal genes. Although further studies are needed to identify the role of other genes in the DA, our data provide a basis for understanding the molecular mechanisms underlying the differentiation and remodeling of the DA and for inventing the novel targets that regulate the contraction of the DA in affected children.

Acknowledgments This work was supported by grants from the Ministry of Health Labor and Welfare (Y.I.), the Ministry of Education, Culture, Sports, Science, and Technology of Japan (Y.I., U.Y., S.M.), the Foundation for Growth Science (S.M.), the Yokohama Foundation for Advanced Medical Science (U.Y., S.M.), the 'High-Tech Research Center' Project for Private Universities: MEXT (S.M.), a Waseda University Grant for Special Research Projects (Q.J.), the Vehicle Racing Commemorative Foundation (S.M.), Miyata Cardiology Research Promotion Funds (U.Y., S.M.), Takeda Science Foundation (Y.I., U.Y., S.M.), the Japan Heart Foundation Research Grant (U.Y.), the Kowa Life Science Foundation (U.Y.),